TRENDS IN SCIENCES 2026; 23(2): 11668
https://doi.org/10.48048/tis.2026.11668 RESEARCH ARTICLE

Microwave-Assisted Synthesis and Antioxidant Evaluation of *α,β*-Unsaturated Ketones Incorporating a Pyrano[3,2-*g*] Chromene-2,6-dione Core via Claisen–Schmidt Condensation

Ngoc Thanh Nguyen*, Thi Thu Giang Pham and Thuy Van Ngo

Faculty of Chemical Technology, Hanoi University of Industry, Tay Tuu Ward, Hanoi, Vietnam

(*Corresponding author's e-mail: thanhnn@haui.edu.vn)

Received: 22 August 2025, Revised: 28 August 2025, Accepted: 4 September 2025, Published: 10 November 2025

Abstract

A green, rapid and high-yielding microwave-assisted synthesis of *α,β*-unsaturated ketones from pyrano[3,2-*g*]chromene derivatives was developed, followed by preliminary structure–activity relationship (SAR) evaluation. Inspired by the broad pharmacological potential of chromone-based scaffolds, these analogues were designed to enhance antioxidant properties. The key intermediate, 7-acetyl-4,8-dimethyl-2*H*,6*H*-pyrano[3,2-*g*]chromene-2,6-dione, was obtained via a Kostanecki–Robinson reaction and subsequently transformed through Claisen–Schmidt condensations with diverse aromatic aldehydes under microwave irradiation, affording twelve target compounds (**6a–6l**) in excellent yields (74% - 95%) within minutes. Structural identities were confirmed by spectroscopic and mass analyses. Antioxidant screening using the DPPH assay identified derivative 6 g as the most potent, exhibiting 86.7% radical scavenging at 50 µM, comparable to ascorbic acid (97.65%). While only a DPPH assay was performed, these results provide preliminary antioxidant insights that warrant further biological validation.

Keywords: *α,β*-unsaturated ketones, Pyranochromones, Pyrano[3,2-*g*]chromene, Claisen–Schmidt condensation, Microwave-assisted synthesis, Green chemistry, Antioxidant activity

Introduction

Chromone derivatives constitute a privileged class of heterocycles with broad pharmacological activities, including antioxidant, anti-inflammatory, antimicrobial and anticancer effects [1,2]. Hybrid chromone frameworks such as styrylchromones further display multipotent profiles against viral, bacterial and tumor targets [3], while multitarget chromone-based agents have been investigated for neurodegenerative disorders, notably Alzheimer's disease, through inhibition of acetylcholinesterase and MAO-B [4-6]. These findings highlight the therapeutic promise of chromone scaffolds but also point to the need for efficient and sustainable synthetic access to novel analogues.

Although traditional methods such as the Claisen condensation, Baker–Venkataraman rearrangement and the Kostanecki–Robinson reaction remain widely employed [7-9], many existing routes still rely on lengthy procedures, hazardous reagents, or generate limited structural diversity. More recent developments—such as metal-catalyzed annulations, solvent-controlled cyclizations and other advanced methodologies [10-15]—have expanded the synthetic toolbox, yet greener and more rapid strategies remain underexplored.

Within this family, the *α*-pyrano[3,2-*g*]chromone framework is particularly attractive due to its rigidity, extended conjugation and reported biological relevance [2]. However, systematic efforts to generate chalcone-type derivatives from this scaffold are scarce and their antioxidant potential has not been fully addressed.

Microwave-assisted organic synthesis (MAOS) offers a sustainable alternative, providing rapid and uniform heating with reduced reaction times and enhanced yields. Its successful application to Claisen–

Schmidt condensations [16-19] positions it as an ideal tool for accessing *α,β*-unsaturated ketones efficiently.

Herein, we describe a green, rapid and high-yielding microwave-assisted synthesis of *α,β*-unsaturated ketones derived from a pyrano[3,2-*g*]chromene-2,6-dione core, followed by preliminary antioxidant evaluation. This work not only demonstrates a concise and sustainable synthetic route but also provides a foundation for exploring the structure–activity relationships of pyranochromene-based chalcones.

Materials and methods

Melting points: Melting points of synthesized compounds were determined using a Stuart SMP3 apparatus and are uncorrected.

Spectroscopic analyses: IR spectra were recorded using KBr pellets on a Nicolet Impact 410 spectrometer. ^{1}H NMR (500 MHz) and ^{13}C NMR (125 MHz) spectra were acquired on a Bruker Avance AV500 spectrometer with DMSO-d_6 as solvent and TMS as internal standard. Due to solubility limitations, full ^{13}C NMR data could not be obtained for some derivatives; in these cases, structural assignments were supported by HSQC and HMBC correlations along with MS and IR evidence. MS spectra were recorded on a Hewlett–Packard 5989B mass spectrometer. Analytical TLC was performed on Merck Kieselgel 60 F_{254} pre-coated plates.

Microwave irradiation: Microwave-assisted reactions were conducted in a CEM Discover SP reactor equipped with infrared temperature monitoring and pressure control.

Chemicals and solvents: All reagents were of analytical grade and used without further purification. Solvents were reagent grade. The synthetic pathway for compounds **3**, **4**, and **6a**–**l** is shown in Scheme 1.

Antioxidant activity assay: The free radical scavenging activity was evaluated using the DPPH assay as previously described [20,21], with minor modifications. Test compounds were dissolved in DMSO at defined concentrations and DPPH was prepared in methanol at an appropriate concentration. An aliquot of 10 µL of each test solution was mixed with 190 µL of the DPPH solution and incubated at 37 °C for 20 min. The absorbance was measured at 517 nm using a UV–vis spectrophotometer (ELISA reader). Ascorbic acid was used as a reference standard to monitor assay stability and compare inhibitory activity. All experiments were performed in triplicate. The percentage of DPPH radical inhibition was calculated using the following equation:

Inhibition of DPPH activity (%) = 100 – [(ODs) / (ODc)×100].

where OD_s is the mean optical density of the sample and ODc is the mean optical density of the control.

Synthesis of compound 4

A solution of compound 3 (0.01 mol) in acetic anhydride (0.10 mol, 9.5 mL) was prepared and sodium acetate (3.0 g) was added as a catalyst. The reaction mixture was refluxed at 130 - 140 °C for 8 h. After cooling, the mixture was poured into 100 g of ice water. The precipitated product was collected by filtration, washed with distilled water and dried. The crude solid was purified by recrystallization from ethanol to afford compound 4. Physical, IR, NMR and MS spectra data of 4 is reported as follows: 7-Acetyl-4,8-dimethyl-2*H*,6*H*-pyrano[3,2-*g*]chromene-2,6-dione 4: Yield 1.22 g (43%) of 4, crystallized from 96% ethanol as pale yellow crystals. Mp 246 - 247 °C. R_f: 0.58 EtOAC/*n*-hexane (2:3, v/v). (IR (KBr, cm^{-1}): 1,735, 1,696 (C=O). ^{1}H NMR (500 MHz, DMSO-d_6) δ: 8.30 (1H, s, H_{benzo}), 7.61 (1H, s, H_{benzo}), 6.48 (1H, s, $H_{\alpha\text{-pyrone}}$), 2.51 (3H, s, $COCH_3$), 2.50 (3H, s, CH_3 $_{\alpha\text{-pyrone}}$) and 2.44 (3H, s, $CH_{3\gamma\text{-pyrone}}$). MS (ESI, m/z): 284 [M]$^+$, 75%; 269 (M^+-CH_3), 100%; 256 (M^+-CO), 241 (269-CO).

Optimization procedure for Claisen–Schmidt condensation

A mixture of 7-acetyl-4,8-dimethyl-2*H*,6*H*-pyrano[3,2-*g*]chromene-2,6-dione (4, 1.0 mmol), *p*-methylbenzaldehyde (5a, 1.2 mmol) and the base catalyst (0.1 mmol) was subjected to different reaction conditions as summarized in **Table 1**.

A. conventional heating under reflux

The reactants were suspended in absolute ethanol (5 mL) and heated under reflux at ~78 °C with vigorous magnetic stirring. The reaction progress was monitored by thin-layer chromatography (TLC) using an ethyl acetate/*n*-hexane mixture (2:3, v/v) as the eluent. Upon

completion, the resulting solid product was collected by filtration, washed thoroughly with cold distilled water and recrystallized from a DMF/EtOH mixture (1:2, v/v) to afford the pure product **6a**.

B. microwave-assisted synthesis in solvent

The mixture was dissolved in the appropriate solvent (5 mL of absolute ethanol or methanol) and transferred into a sealed 10 mL microwave vessel equipped with a magnetic stir bar. The vessel was irradiated in a CEM Discover microwave reactor at a controlled temperature of 120 °C for the specified time (see **Table 1**), with automatic pressure regulation. After the irradiation was complete, the vessel was cooled to room temperature using compressed air and carefully vented. The crude product was isolated and purified as described in method A.

C. microwave-assisted solvent-free synthesis

The solid reactants and base catalyst were placed directly into a clean, dry 10 mL microwave vessel. To ensure efficient mixing and energy transfer, a single drop (~0.05 mL) of absolute ethanol was added (liquid-assisted grinding, LAG). The vessel was sealed and irradiated at 120 °C for the indicated time with constant stirring. The product was isolated and purified as described in method A.

D. conventional heating in a sealed tube

The reaction mixture was dissolved in absolute ethanol (5 mL) and transferred into a heavy-walled glass reaction tube. The tube was sealed under atmosphere and placed into a preheated oil bath at 120 °C for the designated time. After heating, the tube was cooled to ambient temperature, opened carefully and the contents were processed as described in method A.

Yields reported in **Table 1** correspond to isolated, recrystallized products.

General synthesis of 6a–6l

The title compounds **6a**–**6l** were synthesized via a microwave-assisted Claisen–Schmidt condensation according to the optimized conditions established in this study (**Table 1**, Entry 1).

A mixture of 7-acetyl-4,8-dimethyl-2*H*,6*H*-pyrano[3,2-*g*]chromene-2,6-dione (4, 1.0 mmol), the appropriate aromatic aldehyde **5a**–**5l** (1.2 mmol) and piperidine (0.1 mmol, 8.5 μL) in anhydrous ethanol (5 mL) was transferred into a dedicated 10 mL microwave reaction vessel (CEM Discover Series) equipped with a magnetic stir bar. The vessel was sealed and irradiated in the microwave reactor at 120 °C for 10 min, with constant stirring and automatic pressure regulation. The reactor power was automatically adjusted to maintain the set temperature.

Upon completion, the vessel was cooled to ambient temperature (< 40 °C) using compressed air and carefully vented. The resulting precipitate was collected by vacuum filtration, washed thoroughly with cold distilled water (2×5 mL) to remove residual salts and catalyst and dried under reduced pressure.

Further purification was achieved by recrystallization. The crude solid was dissolved in a minimal volume of hot dimethylformamide (DMF). Hot ethanol was then added dropwise to the stirred solution until the point of cloudiness (indicating incipient crystallization). The mixture was allowed to cool slowly to room temperature and subsequently cooled in an ice-water bath for complete crystallization. The purified crystals were isolated by filtration, washed with a small portion of ice-cold ethanol and dried in vacuo to afford the desired *α,β*-unsaturated ketones **6a**–**6l** in high yields and excellent purity, as confirmed by spectroscopic analysis. The physical properties, spectroscopic data (IR, NMR, MS) and specific recrystallization solvent ratios for each compound are provided below:

(*E*)-4,8-dimethyl-7-(3-(*p*-tolyl)acryloyl)-2*H*,6*H*-pyrano[3,2-*g*]chromene-2,6-dione (6a): Yield 0.355 g (92%) of **6a**, crystallized from a mixture of DMF and 96% ethanol (1:2) as bright yellow crystals. Mp 265 - 266 °C. R_f: 0.83. IR (KBr, cm^{-1}): 1,750, 1,689 (C=O), 980 (=CH_{trans} bend.). ^{1}H NMR (500 MHz, DMSO-d_6) δ: 8.34 (1H, s, H_{benzo}), 7.91 (1H, d, *J* = 16.0 Hz, -CH=C*H*-Ar), 7.78 (1H, s, H_{benzo}), 7.59 (2H, d, *J* = 8.0 Hz, Ar-H), 7.30 (2H, d, *J* = 8.0 Hz, Ar-H), 7.10 (1H, d, *J* = 16.0 Hz, -C*H*=CH-Ar), 6.51 (1H, d, *J* = 1.0 Hz, $H_{\alpha\text{-pyrone}}$), 2.59 (3H, s, $CH_{3\gamma\text{-pyrone}}$), 2.53 (3H, d, *J* = 1.0 Hz, $CH_{3\alpha\text{-pyrone}}$), 2.36 (3H, s, Ar-$CH_3$). MS (*m/z*, %): 386 (60.9, M^+), 371 (24.9), 357 (6.2), 343 (29.2), 313 (4.5), 295 (60.5), 281 (23.8), 267 (8.8), 259 (5.0), 255 (1.5), 253 (4.1), 241 (4.5), 239 (8.0), 238 (4.6), 229 (7.0), 203 (13.1), 202 (8.5), 193 (8.1), 189 (6.6), 175 (7.8), 174 (7.6), 171 (8.9), 157 (11.6), 147 (4.3), 146 (11.0), 141 (42.1), 139

(28.4), 138 (5.0), 115 (100), 97 (20.2), 91 (32.7), 90 (18.3), 57 (71.1), 55 (80.0).

(*E*)-7-(3-(4-bromophenyl)acryloyl)-4,8-dimethyl-2*H*,6*H*-pyrano[3,2-*g*]chromene-2,6-dione (**6b**): Yield 0.405 g (90%) of **6b**, crystallized from a mixture of DMF and 96% ethanol (1:1) as yellow crystals. Mp 334 - 335 °C. R_f: 0.62. IR (KBr, cm^{-1}): 1,748, 1,677 (C=O), 967 (=CH_{trans} bend.). ^{1}H NMR (500 MHz, DMSO-d_6) δ: 8.33 (1H, s, H_{benzo}), 7.90 (1H, d, J = 16.0 Hz, -CH=C*H*-Ar), 7.76 (1H, s, H_{benzo}), 7.66 (2H, d, J = 8.0 Hz, Ar-H), 7.15 (1H, d, J = 16.0 Hz, -C*H*=CH-Ar), 6.51 (1H, s, $H_{\alpha\text{-pyrone}}$), 2.59 (3H, s, $CH_{3\gamma\text{-pyrone}}$), 2.53 (3H, s, $CH_{3\alpha\text{-pyrone}}$). MS (*m/z*, %): 452/450 (31.0, M^+), 435 (9.4), 409 (7.1), 396 (1.6), 371 (12.4), 353 (2.8), 342 (6.1), 313 (4.0), 295 (100), 281 (40.6), 267 (12.1), 259 (1.1), 255 (3.8), 253 (4.0), 241 (2.0), 239 (8.1), 238 (2.5), 215 (16.3), 203 (15.4), 202 (9.0), 189 (8.3), 185 (5.7), 175 (10.0), 174 (12.1), 154 (33.1), 147 (6.3), 146 (10.4), 139 (12.2), 138 (3.1), 126 (84.6), 115 (14.3), 102 (18.25), 91 (11.6), 90 (20.8), 84 (29.3), 66 (42.7), 57 (37.8), 55 (16.5).

(*E*)-4,8-dimethyl-7-(3-(4-nitrophenyl)acryloyl)-2*H*,6*H*-pyrano[3,2-*g*]chromene-2,6-dione (**6c**): Yield 0.396 g (95%) of **6c**, crystallized from a mixture of DMF and 96% ethanol (1:1) as yellow crystals. Mp 321 - 322 °C. R_f: 0.73. IR (KBr, cm^{-1}): 1,760, 1,695 (C=O), 1,505 (NO_2 asym.), 1,350 (NO_2 sym.), 954 (=CH_{trans} bend.). ^{1}H NMR (500 MHz, DMSO-d_6) δ: 8.37 (1H, s, H_{benzo}), 8.31 (2H, d, J = 8.5 Hz, Ar-H), 8.04 (1H, d, J = 16.0 Hz, -CH=C*H*-Ar), 7.99 (2H, d, J = 8.5 Hz, Ar-H), 7.79 (1H, s, H_{benzo}), 7.33 (1H, d, J = 16.0 Hz, -C*H*=CH-Ar), 6.53 (1H, s, $H_{\alpha\text{-pyrone}}$), 2.61 (3H, s, $CH_{3\gamma\text{-pyrone}}$), 2.55 (3H, s, $CH_{3\alpha\text{-pyrone}}$). MS (*m/z*, %): 417 (48.8, M^+), 402 (12.9), 387 (18.3), 370 (19.1), 342 (11.6), 313 (13.8), 295 (100), 281 (32.1), 267 (9.9), 259 (5.5), 255 (4.1), 239 (16.0), 238 (7.4), 215 (9.1), 203 (14.5), 202 (12.6), 189 (8.9), 185 (10.4), 175 (17.7), 174 (10.7), 147 (7.1), 146 (12.2), 139 (18.1), 126 (52.1), 115 (35.4), 91 (25.9), 90 (29.6), 89 (42.3), 69 (46.5), 57 (57.6), 55 (50.1).

(*E*)-4,8-dimethyl-7-(3-(3-nitrophenyl)acryloyl)-2*H*,6*H*-pyrano[3,2-*g*]chromene-2,6-dione (**6d**): Yield 0.366 g (89%) of **6d**, crystallized from a mixture of DMF and 96% ethanol (1:1) as yellow crystals. Mp 324 - 325 °C. R_f: 0.40. IR (KBr, cm^{-1}): 1,744, 1,682 (C=O), 1,535 (NO_2 asym.), 1,370 (NO_2 sym.), 972 (=CH_{trans} bend.). ^{1}H NMR (500 MHz, DMSO-d_6) δ: 8.53 (1H, s, Ar-H), 8.36 (1H, s, H_{benzo}), 8.26 (1H, d, J = 8.5 Hz, Ar-H), 8.18 (1H, d, J = 8.0 Hz, Ar-H), 8.09 (1H, d, J = 16.0 Hz, -CH=C*H*-Ar), 7.76 (1H, t, J = 8.5, 8.0 Hz, Ar-H), 7.76 (1H, s, H_{benzo}), 7.31 (1H, d, J = 16.0 Hz, -C*H*=CH-Ar), 6.52 (1H, s, $H_{\alpha\text{-pyrone}}$), 2.60 (3H, s, $CH_{3\gamma\text{-pyrone}}$), 2.53 (3H, s, $CH_{3\alpha\text{-pyrone}}$). MS (*m/z*, %): 417 (41.2, M^+), 402 (7.2), 387 (2.4), 370 (4.5), 344 (14.7), 328 (5.4), 295 (100), 281 (23.5), 267 (17.1), 259 (3.3), 255 (2.6), 253 (3.5), 239 (6.8), 238 (1.5), 215 (10.4), 203 (10.8), 202 (13.5), 189 (10.2), 175 (8.5), 174 (8.6), 147 (4.9), 146 (15.6), 139 (14.6), 138 (2.4), 126 (61.1), 115 (24.1), 91 (11.2), 90 (29.3), 89 (31.2), 69 (17.8), 57 (8.6), 55 (11.5).

(*E*)-4,8-dimethyl-7-(3-(2-nitrophenyl)acryloyl)-2*H*,6*H*-pyrano[3,2-*g*]chromene-2,6-dione (**6e**): Yield 0.350 g (84%) of **6e**, crystallized from a mixture of DMF and 96% ethanol (1:1) as pale yellow crystals. Mp 317 - 318 °C. R_f: 0.64. IR (KBr, cm^{-1}): 1,765, 1,690 (C=O), 1,520 (NO_2 asym.), 1,380 (NO_2 sym.), 963 (=CH_{trans} bend.). ^{1}H NMR (500 MHz, DMSO-d_6) δ: 8.30 (1H, s, H_{benzo}), 8.14 (1H, d, J = 16.0 Hz, -CH=C*H*-Ar), 8.10 (1H, d, J = 8.0 Hz, Ar-H), 7.89 (1H, d, J = 7.5 Hz, Ar-H), 7.83 (1H, t, J = 7.5, 7.5 Hz, Ar-H), 7.75 (1H, s, H_{benzo}), 7.70 (1H, t, J = 8.0, 7.5 Hz, Ar-H), 7.11 (1H, d, J = 16.0 Hz, -C*H*=CH-Ar), 6.53 (1H, s, $H_{\alpha\text{-pyrone}}$), 2.60 (3H, s, $CH_{3\gamma\text{-pyrone}}$), 2.52 (3H, s, $CH_{3\alpha\text{-pyrone}}$). MS (*m/z*, %): 417 (11.4, M^+), 402 (8.0), 386 (3.7), 370 (77.5), 342 (33.0), 328 (16.7), 295 (36.0), 281 (44.6), 267 (6.9), 259 (9.6), 255 (49.3), 253 (23.7), 239 (10.2), 226 (25.6), 210 (38.3), 203 (35.3), 202 (25.3), 189 (20.3), 187 (21.0), 174 (36.0), 147 (14.2), 146 (28.4), 139 (33.7), 138 (5.7), 126 (68.0), 115 (60.4), 91 (62.9), 90 (82.9), 89 (97.5), 77 (100), 69 (74.8), 57 (62.0), 55 (51.7).

(*E*)-4,8-dimethyl-7-(3-(4-hydroxyphenyl)acryloyl)-2*H*,6*H*-pyrano[3,2-*g*]chromene-2,6-dione (**6f**): Yield 0.318 g (82%) of **6f**, crystallized from a mixture of DMF and 96% ethanol (1:1) as yellow crystals. Mp 321 - 322 °C. R_f: 0.44. IR (KBr, cm^{-1}): 3295 (OH), 1,731, 1,693 (C=O), 980 (=CH_{trans} bend.). ^{1}H NMR (500 MHz, DMSO-d_6) δ: 10.20 (1H, s, Ar-OH), 8.30 (1H, s, H_{benzo}), 7.84 (1H, d, J = 16.0 Hz, -CH=C*H*-Ar), 7.74 (1H, s, H_{benzo}), 7.54 (2H, d, J = 8.5 Hz. Ar-H), 6.86 (2H, d, J = 8.5 Hz, Ar-H), 6.64 (1H, d, J = 16.0 Hz, -C*H*=CH-Ar), 6.49 (1H, s, $H_{\alpha\text{-pyrone}}$), 2.58 (3H, s, $CH_{3\gamma\text{-pyrone}}$), 2.52 (3H, s, $CH_{3\alpha\text{-pyrone}}$). MS (*m/z*, %): 388 (80.6, M^+), 373 (27.7), 359 (8.8), 345 (29.1), 317 (4.0), 295 (52.3), 281 (28.3), 267

(10.1), 259 (2.6), 255 (5.0), 253 (3.6), 239 (6.6), 238 (3.1), 203 (22.7), 202 (11.8), 189 (14.8), 175 (13.5), 174 (8.7), 171 (25.8), 157 (13.9), 147 (11.4), 146 (11.4), 143 (41.0), 139 (13.1), 138 (3.1), 115 (100), 97 (22.3), 91 (23.6), 90 (32.5), 89 (36.5), 77 (40.6), 57 (57.3), 55 (66.8).

(*E*)-7-(3-(4-hydroxy-3-methoxyphenyl)acryloyl)-4,8-dimethyl-2*H*,6*H*-pyrano[3,2-*g*]chromene-2,6-dione (**6g**): Yield 0.334 g (80%) of **6g**, crystallized from a mixture of DMF and 96% ethanol (1:2) as yellow crystals. Mp 297 - 298 °C. R_f: 0.57. IR (KBr, cm^{-1}): 3,425 (OH), 1,723 (C=O), 967 (=CH_{trans} bend.). ^{1}H NMR (500 MHz, DMSO-d_6) δ: 9.77 (1H, s, Ar–OH), 8.35 (1H, s, Hb_{enzo}), 7.90 (1H, d, J = 16.0 Hz, –CH=C*H*–Ar), 7.88 (1H, d, J = 8.0 Hz, Ar–H), 7.78 (1H, s, H_{benzo}), 7.25 (1H, s, Ar–H), 7.21 (1H, d, J = 8.0 Hz, Ar–H), 6.98 (1H, d, J = 16.0 Hz, –C*H*=CH–Ar), 6.52 (1H, s, $H_{α\text{-pyrone}}$), 3.86 (3H, s, Ar–OMe), 2.59 (3H, s, $CH_{3\ γ\text{-pyrone}}$), 2.54 (3H, s, $CH_{3\ α\text{-pyrone}}$).

(*E*)-7-(3-(2-hydroxyphenyl)acryloyl)-4,8-dimethyl-2*H*,6*H*-pyrano[3,2-*g*]chromene-2,6-dione (**6h**): Yield 0.302 g (78%) of **6h**, crystallized from a mixture of DMF and 96% ethanol (1:1) as yellow crystals. Mp 254 - 255 °C. R_f: 0.43. IR (KBr, cm^{-1}): 3,249 (OH), 1,739, 1,696 (C=O), 960 (=CH_{trans} bend.). ^{1}H NMR (500 MHz, DMSO-d_6) δ: 10.40 (1H, s, Ar–OH), 8.34 (1H, s, H_{benzo}), 8.04 (1H, d, J = 16.0 Hz, –CH=C*H*–Ar), 7.82 (1H, s, H_{benzo}), 7.55 (1H, d, J = 7.0 Hz, Ar–H), 7.31 (1H, d, J = 16.0 Hz, –C*H*=CH–Ar), 7.25 (1H, t, J = 8.0, 7.0 Hz, Ar–H), 6.94 (1H, d, J = 8.0 Hz, Ar–H), 6.89 (1H, t, J = 8.0, 7.0 Hz, Ar–H), 6.51 (1H, s, $H_{α\text{-pyrone}}$), 2.57 (3H, s, $CH_{3\ γ\text{-pyrone}}$), 2.53 (3H, s, $CH_{3\ α\text{-pyrone}}$). ^{13}C-NMR (125 MHz, DMSO-d_6) δ: 200.2, 174.6, 161.2, 158.9, 157.1, 156.5, 156.0, 152.7, 136.5, 129.6, 122.9, 121.9, 121.5, 119.7, 119.6, 118.2, 117.1, 116.4, 114.8, 113.9, 105.3, 32.09, 18.18. MS (*m/z*, %): 388 (14.2, M^+), 369 (4.1), 345 (100), 295 (8.0), 281 (4.0), 269 (4.5), 239 (4.4), 203 (11.1), 202 (7.3), 189 (8.1), 175 (14.7), 174 (8.2), 171 (96.7), 157 (6.1), 147 (8.9), 146 (9.6), 144 (59.7), 115 (65.2), 97 (21.2), 91 (31.6), 90 (16.6), 89 (34.2), 77 (40.5), 57 (44.4), 55 (51.4).

(*E*)-7-(3-(benzo[*d*][1,3]dioxol-5-yl)acryloyl)-4,8-dimethyl-2*H*,6*H*-pyrano[3,2-*g*]chromene-2,6-dione (**6i**): Yield 0.345 g (83%) of **6i**, crystallized from a mixture of DMF and 96% ethanol (1:1) as yellow crystals. Mp 312 - 313 °C. R_f: 0.75. IR (KBr, cm^{-1}): 1,758, 1,683 (C=O), 953 (=CH_{trans} bend.). ^{1}H NMR (500 MHz, DMSO-d_6) δ: 8.32 (1H, s, H_{benzo}), 7.84 (1H, d, J = 16.0 Hz, –CH=C*H*–Ar), 7.73 (1H, s, H_{benzo}), 7.33 (1H, s, Ar–H), 7.21 (1H, d, J = 8.0 Hz, Ar–H), 7.01 (1H, d, J = 8.0 Hz, Ar–H), 6.98 (1H, d, J = 16.0 Hz, –C*H*=CH–Ar), 6.50 (1H, s, $H_{α\text{-pyrone}}$), 6.10 (2H, s, –CH_2–), 2.58 (3H, s, $CH_{3\ γ\text{-pyrone}}$), 2.52 (3H, s, $CH_{3\ α\text{-pyrone}}$). MS (*m/z*, %): 416 (83.2, M^+), 401 (24.1), 373 (73.1), 357 (13.0), 345 (6.8), 315 (28.2), 295 (62.2), 281 (31.1), 267 (11.6), 259 (19.2), 255 (2.0), 253 (2.9), 239 (7.2), 238 (2.9), 203 (23.3), 189 (14.2), 175 (15.3), 174 (12.2), 169 (50.6), 141 (28.0), 139 (10.6), 138 (4.6), 113 (100), 89 (48.2), 63 (42.5), 57 (26.3), 55 (27.6).

(*E*)-7-(3-(furan-2-yl)acryloyl)-4,8-dimethyl-2*H*,6*H*-pyrano[3,2-*g*]chromene-2,6-dione (**6j**): Yield 0.267 g (74%) of **6j**, crystallized from a mixture of DMF and 96% ethanol (1:1) as pale yellow crystals. Mp 267 - 268 °C. R_f: 0.60. IR (KBr, cm^{-1}): 1,746, 1,667 (C=O), 974 (=CH_{trans} bend.). ^{1}H NMR (500 MHz, DMSO-d_6) δ: 8.32 (1H, s, H_{benzo}), 7.92 (1H, d, J = 1.5 Hz, Ar–H), 7.75 (1H, d, J = 16.0 Hz, –CH=C*H*–Ar), 7.72 (1H, s, H_{benzo}), 6.99 (1H, d, J = 3.5 Hz, Ar–H), 6.94 (1H, d, J = 16.0 Hz, –C*H*=CH–Ar), 6.70 (1H, dd, J = 3.5, 1.5 Hz, Ar–H), 6.49 (1H, d, J = 1.0 Hz, H $_{α\text{-pyrone}}$), 2.58 (3H, s, $CH_{3\ γ\text{-pyrone}}$), 2.52 (3H, d, J = 1.0 Hz, $CH_{3\ α\text{-pyrone}}$). ^{13}C NMR (125 MHz, DMSO-d_6) δ: 200.2, 174.6, 160.7, 158.9, 156.5, 156.0, 152.7, 151.0, 146.6, 127.1, 123.0, 121.8, 119.8, 118.2, 116.8, 114.8, 114.3, 113.3, 105.2, 32.04, 18.19. MS (*m/z*, %): 362 (49.3, M^+), 344 (8.3), 333 (19.9), 319 (11.6), 305 (11.3), 295 (2.9), 291 (13.8), 281 (26.1), 267 (3.3), 263 (10.6), 257 (3.5), 253 (6.8), 239 (7.3), 238 (2.6), 203 (10.6), 202 (3.3), 189 (3.5), 175 (8.0), 174 (7.0), 169 (5.4), 165 (7.3), 145 (31.1), 139 (10.2), 138 (6.5), 129 (19.2), 111 (16.9), 97 (30.5), 91 (13.4), 90 (26.7), 89 (61.8), 69 (72.3), 57 (87.4), 55 (100).

(*E*)-7-(3-(1*H*-indol-3-yl)acryloyl)-4,8-dimethyl-2*H*,6*H*-pyrano[3,2-*g*]chromene-2,6-dione (**6k**): Yield 0.345 g (84%) of **6k**, crystallized from a mixture of DMF and 96% ethanol (1:1) as yellow crystals. Mp 326 - 327 °C. R_f: 0.49. IR (KBr, cm^{-1}): 3,295 (N-H), 1,712, 1,674 (C=O), 945 (=CH_{trans} bend.). ^{1}H NMR (500 MHz, DMSO-d_6) δ: 12.21 (1H, s, NH), 8.25 (1H, s, H_{benzo}), 8.10 (1H, d, J = 16.0 Hz, –CH=C*H*–Ar), 8.01 (1H, s, Ar–H), 7.84 (1H, d, J = 6.5 Hz, Ar–H), 7.70 (1H, s, H_{benzo}), 7.60 (1H, d, J = 6.5 Hz, Ar–H), 7.37 (1H, d, J = 16.0 Hz, –C*H*=CH–Ar), 7.28 (1H, t, J = 6.5, 6.5 Hz, Ar–

H), 6.43 (1H, s, H $_{\alpha\text{-pyrone}}$), 2.59 (3H, s, CH_3 $_{\gamma\text{-pyrone}}$), 2.47 (3H, s, CH_3 $_{\alpha\text{-pyrone}}$).

(*E*)-4,8-dimethyl-7-(3-(1-methyl-1*H*-indol-3-yl)acryloyl)-2*H*,6*H*-pyrano[3,2-*g*]chromene-2,6-dione (**6l**): Yield 0.344 g (81%) of **6l**, crystallized from a mixture of DMF and 96% ethanol (1:1) as yellow crystals. Mp 324 - 325 °C. R_f: 0.41. IR (KBr, cm^{-1}): 1,719, 1,670 (C=O), 956 (=CH_{trans} bend.). ^{1}H NMR (500 MHz, DMSO-d_6) δ: 8.36 (1H, s, H_{benzo}), 8.21 (1H, d, *J* = 16.0 Hz, –CH=C*H*–Ar), 8.04 (1H, s, Ar–H), 7.91 (1H, d, *J* = 7.0 Hz, Ar–H), 7.80 (1H, s, H_{benzo}), 7.59 (1H, d, *J* = 7.0 Hz, Ar–H), 7.33 (1H, t, *J* = 7.0, 7.0 Hz, Ar–H), 7.25 (1H, d, *J* = 16.0 Hz, –C*H*=CH–Ar), 6.51 (1H, s, H $_{\alpha\text{-pyrone}}$), 3.89 (1H, s, NCH_3), 2.62 (3H, s, CH_3 $_{\gamma\text{-pyrone}}$), 2.54 (3H, s, CH_3 $_{\alpha\text{-pyrone}}$).

Results and discussion

6-Acetyl-7-hydroxy-4-methylcoumarin (**3**) was prepared according to our previously reported procedure [22,23] by cyclocondensation of 2,4-dihydroxyacetophenone (**1**) with ethyl acetoacetate (**2**) in nitrobenzene, catalyzed by $POCl_3$ at room temperature for seven days (Scheme 2, step *a*), affording a 25.9% yield.

7-Acetyl-4,8-dimethyl-2*H*,6*H*-pyrano[3,2-*g*]chromene-2,6-dione (**4**) was synthesized via a Kostanecki–Robinson cyclocondensation of 6-acetyl-7-hydroxy-4-methylcoumarin (**3**) with acetic anhydride in the presence of sodium acetate (Scheme 1, step *b*). Sodium acetate deprotonates the *α*-position of the C-6 acetyl group to generate an enolate, which undergoes C-acylation with acetic anhydride to afford an *α*-acylated ketone. Subsequent O-acetylation of the C-7 hydroxyl group enables intramolecular nucleophilic attack of the enolate on the O-acetyl carbonyl, leading to cyclization and dehydration to furnish the fused *γ*-pyrone ring. Thus, sodium acetate promotes both enolate formation and acyl transfer, whereas acetic anhydride serves as the acetylating, activating and dehydrating agent [23]. The structure of compound **4** was confirmed by ^{1}H and ^{13}C NMR, IR and MS data, consistent with our previous report [24].

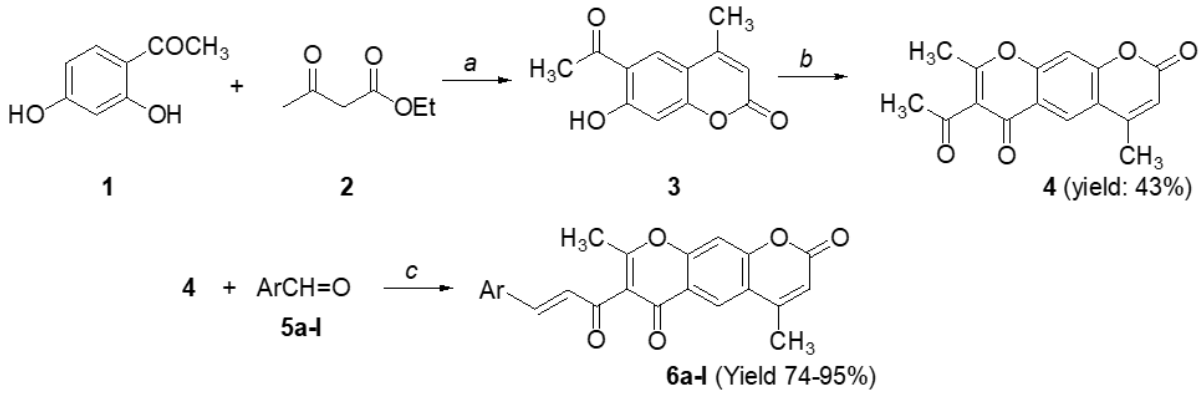

Scheme 1 Synthetic route to compounds **6a**–**l** from 2,4-dihydroxyacetophenone. Reaction conditions: (*a*) $POCl_3$, nitrobenzene, rt, 7 days; (*b*) $(CH_3CO)_2O$, AcONa (cat.), reflux, 8 h; (*c*) piperidine (cat.), EtOH, microwave, 120 °C, 10 min.

The optimization results for the Claisen-Schmidt condensation between ketone **4** and *p*-methylbenzaldehyde **5a** to form the chalcone analog **6a** (**Table 1**) provide a compelling case for the superiority of specific reaction conditions, with Entry 1 emerging as the unequivocal optimum.

The critical role of the base catalyst is immediately apparent. The stark contrast between the excellent yield obtained with piperidine (92%, Entry 1) and the poor performance of sodium hydroxide (60%, Entry 3) is the most telling comparison. This discrepancy is not merely a matter of efficiency but of chemical compatibility. The chromene-dione scaffold of compound **4** contains a

highly base-sensitive lactone ring. The strong, aqueous nature of NaOH is notorious for catalyzing the hydrolytic ring-opening of such lactones, leading to structural decomposition and a complex mixture of side products, which drastically diminishes the isolated yield of **6a** [25]. In contrast, piperidine, a milder organic base, provides sufficient basicity to deprotonate the activated methyl ketone and generate the reactive enolate intermediate without causing extensive degradation of the acid-sensitive lactone, leading to a cleaner reaction profile and a superior yield [26].

The method of energy input is another decisive factor. Microwave irradiation (MW) consistently outperforms conventional heating. The dramatic reduction in reaction time from 180 min under conventional reflux (Entry 4, 68%) to a mere 10 min under MW (Entry 1, 92%) highlights the kinetic advantage of this approach. Microwave dielectric heating provides instantaneous, volumetric and homogeneous energy transfer, eliminating thermal gradients and ensuring the entire reaction mixture rapidly reaches the set temperature [27]. The control experiment in Entry 7 is particularly revealing: heating an identical mixture in a sealed tube within an oil bath at the same temperature and for the same duration as Entry 1 resulted in a significantly lower yield (78% vs. 92%). This result suggests that the rate enhancement under microwave irradiation may not be attributable solely to thermal transfer but rather to the highly efficient and rapid heating characteristics of microwave energy, which collectively promote the desired reaction pathway [27].

Furthermore, the high efficiency of the solvent-free approach (Entry 6, 82%, 4 min) demonstrates a powerful and sustainable alternative. The extremely high concentration of reactants under neat conditions maximizes collision frequency, while microwave irradiation provides efficient energy transfer. This protocol aligns perfectly with the principles of green chemistry by eliminating the environmental and economic costs associated with solvent use [28].

In conclusion, this optimization study definitively identifies the conditions in Entry 1—employing piperidine as a base catalyst in ethanol under microwave irradiation at 120 °C for 10 min—as the optimal protocol for this Claisen-Schmidt condensation. This combination successfully balances high catalytic efficiency with substrate stability, leveraging the unique advantages of microwave heating to achieve a reaction that is not only high-yielding (92%) but also exceptionally rapid. The developed method provides a robust, reliable and efficient foundation for the synthesis of compound **6a** and analogous structures.

Table 1 Optimization of reaction conditions for the synthesis of compound 6a.

Entry	Base	Solvent	Conditions	Temp (°C)	Time (min)	Yield (%)
1	Piperidine	EtOH	Microwave irradiation	120	10	92 ± 0.8
2	Et_3N	EtOH	Microwave irradiation	120	15	72 ± 1.1
3	NaOH	EtOH	Microwave irradiation	100	20	60 ± 0.8
4	Piperidine	EtOH	Conventional reflux	~78	180	68 ± 0.9
5	Piperidine	MeOH	Microwave irradiation	120	10	84 ± 1.0
6	Piperidine	Neat	Microwave irradiation	120	4	82 ± 1.3
7	Piperidine	EtOH	Sealed tube, oil bath	120	10	78 ± 0.9

With the optimal conditions established (**Table 1**), we next explored the substrate scope by examining a series of aromatic aldehydes with diverse electronic and steric properties (**Table 2**). In general, electron-deficient aldehydes, such as 4-nitrobenzaldehyde (**6c**, 95%) and 4-bromobenzaldehyde (**6b**, 90%), afforded higher yields compared to electron-rich substrates, such as vanillin (**6g**, 80%), consistent with the expected enhancement in electrophilicity of the carbonyl group. Heteroaromatic aldehydes, including furfural (**6j**, 74%) and indole-3-carbaldehyde (**6k**, 84%), were also well tolerated, while sterically hindered aldehydes such as 2-hydroxybenzaldehyde (**6h**, 78%) exhibited only a modest decrease in yield. These results reveal clear

electronic and steric trends across the substrate series, although a full quantitative analysis of substituent effects (e.g., Hammett correlations) is beyond the scope of the present study and will be the subject of future work.

These findings are consistent with previous reports on microwave-assisted Claisen–Schmidt condensations [29-31], where dielectric heating accelerates reaction rates and suppresses side reactions. In contrast to earlier protocols that required stronger bases or prolonged heating [31,32], our method employs ethanol as a green solvent under mild base conditions, achieving yields of up to 95% within minutes. All products (**6a**–**l**) were obtained exclusively as the (*E*)-isomers, stabilized by extended π-conjugation between the chromene core and the enone moiety.

Table 2 Microwave-assisted synthesis of *α,β*-unsaturated ketones (**6a**–**l**).

Entry	Aldehyde	Product	R_f	Yield (%)	Mp (°C)
1	*p*-Methylbenzaldehyde	6a	0.83	92 ± 0.8	265 - 266
2	*p*-Bromobenzaldehyde	6b	0.62	90 ± 1.0	334 - 335
3	*p*-Nitrobenzaldehyde	6c	0.73	95 ± 0.8	321 - 322
4	*m*-Nitrobenzaldehyde	6d	0.40	89 ± 0.9	324 - 325
5	*o*-Nitrobenzaldehyde	6e	0.64	84 ± 1.0	317 - 318
6	4-Hydroxybenzaldehyde	6f	0.44	82 ± 0.6	321 - 322
7	Vanillin	6g	0.57	80 ± 0.7	297 - 298
8	2-Hydroxybenzaldehyde	6h	0.43	78 ± 1.0	254 - 255
9	3,4-Dimethoxybenzaldehyde	6i	0.75	83 ± 0.9	312 - 313
10	Furfural	6j	0.60	74 ± 1.0	267 - 268
11	Indol-3-carbaldehyde	6k	0.49	84 ± 1.2	326 - 327
12	N-Methylindole-3-carbaldehyde	6l	0.41	81 ± 0.9	324 - 325

The *α,β*-unsaturated ketones **6a**–**l** were fully characterized by IR, ^{1}H NMR, ^{13}C NMR (selected examples) and mass spectrometry.

The IR spectra of **6a**–**l** exhibited *α*-pyrone C=O absorptions at 1,712 - 1,765 cm^{-1} and overlapping *γ*-pyrone/*α,β*-unsaturated ketone C=O bands at 1,667 - 1,696 cm^{-1}. A strong band at 945 - 980 cm^{-1} confirmed the (*E*)-geometry, while substituent-specific absorptions (e.g., NO_2, O–H, N–H) further supported the proposed structures.

The ^{1}H NMR spectra showed two well-resolved vinylic doublets ($J \approx 16.0$ Hz), confirming the (*E*)-geometry of the enone system. Across the series, H-*β* consistently resonated more downfield (δ 7.75 - 8.21) than H-*α* (δ 6.64 - 7.37). H-*β* chemical shifts correlated with the electronic nature of the aryl substituents: electron-withdrawing groups (e.g., NO_2 in **6c**–**e**, δ ≥ 8.04; Br in **6b**, δ 7.90) induced downfield shifts, whereas electron-donating groups (e.g., OH in **6f**, δ 7.84; OMe/OH in **6g**, δ 7.90) produced upfield shifts. Heteroaryl substituents had variable effects, with 2-furyl (**6j**, δ 7.75) being the most upfield and indolyl derivatives (**6k**, δ 8.10; **6l**, δ 8.21) being the most downfield. In contrast, H-*α* resonances exhibited less variation, likely because the adjacent carbonyl group dominates their chemical environment and their greater spatial separation from aryl substituents reduces substituent effects.

The ^{13}C NMR spectra of representative derivatives **6h** and **6j** displayed three characteristic carbonyl resonances: *α,β*-unsaturated ketone C=O (~200.2 ppm), *γ*-lactone (~174.6 ppm) and *α*-pyrone (~158.9 ppm). Additional resonances included oxygenated/quaternary sp² carbons (δ C 150 - 162), the pyrone-ring CH (~105 ppm) and two methyl carbons (δ C 32.0 and 18.2 ppm).

The similarity of these data between **6h** and **6j** confirmed structural consistency across the series.

To further substantiate these assignments, HSQC and HMBC analyses were performed. In the HSQC spectrum, one-bond $^{1}H–^{13}C$ correlations enabled the unambiguous assignment of all protonated carbons. The *α*-pyrone proton (δ H ~6.51 ppm) correlated directly with δ C ~114.8 ppm, while the *β*-vinylic proton (δ H ~8.04 ppm) correlated with δ C ~136.5 ppm.

The HMBC spectrum provided long-range $^{1}H–^{13}C$ correlations, confirming the connectivity of the chromone core and the substitution pattern. Key correlations included the *α*-pyrone proton with carbons at δ C ~117.1 and δ C ~158.9 (carbonyl), and the *β*-vinylic proton with multiple aromatic/quaternary carbons (δ C ~116.4, 129.6, 157.1, 161.2), supporting the placement of substituents on the chromone scaffold.

These HSQC and HMBC results for 6h are representative of the pyrano[3,2-*g*]chromene derivatives **6a**–**6l**. Full spectra of 6h are provided in the Supplementary Information.

EI-MS spectra of **6a**–**l** exhibited molecular ions $[M]^{+}$ consistent with calculated masses; halogenated derivatives (e.g., **6b**) showed the expected isotopic patterns. A fragment at m/z 295, arising from aryl cleavage of the enone side chain to give a conjugated acylium–vinyl cation, was detected in several derivatives and constituted the base peak in some cases, reflecting its enhanced stability under EI conditions. Sequential fragments at m/z 269 and 241, corresponding to further neutral losses, were also observed. Substituent-specific features, such as M−46 (NO_2 loss) for nitro analogues, were likewise evident. Collectively, the fragmentation patterns together with the molecular ions strongly support the proposed structures (**Scheme 2**).

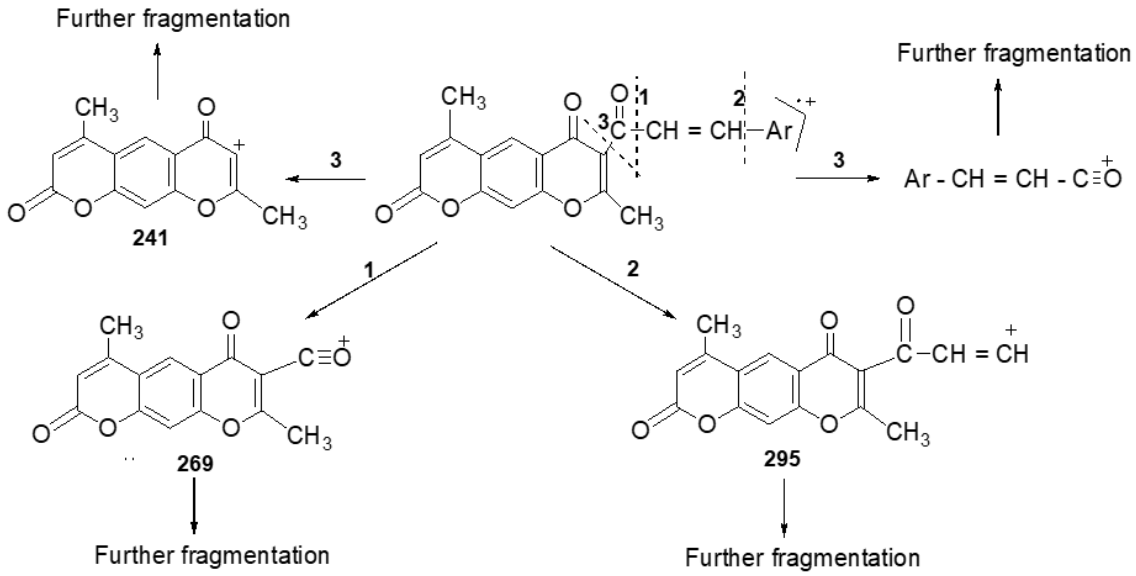

Scheme 2 General fragmentation of **6a**-**l**.

Collectively, the large trans-vinylic coupling constants, characteristic carbonyl IR absorptions, and diagnostic mass fragments unambiguously confirm the structures and *E*-geometry of **6a**-**l**.

The antioxidant screening of compounds **6a**–**6l** suggests a potential structure-activity relationship (SAR), with the phenolic hydroxyl group appearing to play an important role in radical scavenging activity (**Table 3**).

Among the series, the vanillin derivative **6g** (86.67% inhibition at 50 μM) and the 4-hydroxybenzaldehyde derivative 6f (68.56%) exhibited relatively strong, dose-dependent activity, approaching that of the standard antioxidant ascorbic acid (97.65%). This activity is likely related to the ability of phenolic compounds to donate hydrogen atoms to free radicals, thereby stabilizing them and terminating oxidative chain propagation [33]. In contrast, derivatives lacking this

hydrogen-donating group (6a–6e, 6h–6l, all < 45% inhibition at 50 μM) showed markedly lower activity, providing a preliminary negative control and indicating that electronic effects or other substituents alone may not be sufficient to confer significant antioxidant potency [34]. It is noteworthy, however, that even among the phenolic derivatives, a significant activity difference was observed between the ortho- and para-isomers. The significant lower activity of the 2-hydroxy derivative **6h** (43.33%) compared to its 4-hydroxy analogue **6f** (68.56%) can be rationalized by the influence of intramolecular hydrogen bonding (IHB). The ortho-hydroxy group in **6h** likely forms a strong IHB with the adjacent carbonyl oxygen, which reduces its ability to donate a hydrogen atom to the DPPH radical, thereby lowering its antioxidant efficacy compared to the para-isomer 6f where no such IHB exists and the phenolic OH is freely available [35].

These findings are consistent with general principles of antioxidant chemistry, which emphasize the importance of hydrogen-donating ability in radical scavenging [33,34]. Based on this initial screening, compounds 6g and 6f emerge as initial candidates showing potential antioxidant activity; however, further investigation through broader antioxidant assays (such as ABTS, FRAP, or ORAC to evaluate different mechanistic pathways [36-38]) and mechanistic studies is necessary to fully evaluate their therapeutic potential.

Table 3 Inhibition (%) of test compounds.

Compound	Aldehyde	% Inhibition (10 μM)	% Inhibition (50 μM)
Ascorbic acid	–	40.49 ± 2.27	97.65 ± 0.10
6a	*p*-Methylbenzaldehyde	8.23 ± 0.16	24.29 ± 0.29
6b	*p*-Bromobenzaldehyde	6.17 ± 0.11	22.00 ± 0.20
6c	*p*-Nitrobenzaldehyde	8.96 ± 0.20	18.69 ± 0.22
6d	*m*-Nitrobenzaldehyde	6.64 ± 0.24	9.43 ± 0.24
6e	*o*-Nitrobenzaldehyde	7.64 ± 0.30	16.69 ± 0.12
6f	4-Hydroxybenzaldehyde	30.00 ± 1.00	68.56 ± 1.11
6g	Vanillin	36.57 ± 1.43	86.67 ± 1.33
6h	2-Hydroxybenzaldehyde	19.09 ± 0.45	43.33 ± 0.67
6i	3,4-Dimethoxybenzaldehyde	18.67 ± 0.33	36.32 ± 0.53
6j	Furfural	4.26 ± 0.21	18.18 ± 0.36
6k	Indol-3-carbaldehyde	14.09 ± 0.45	38.33 ± 0.67
6l	N-Methylindole-3-carbaldehyde	8.17 ± 0.11	22.00 ± 0.20

Conclusions

A series of novel *α,β*-unsaturated ketones bearing a pyrano[3,2-*g*]chromene-2,6-dione core (**6a**–**l**) was efficiently synthesized via a microwave-assisted Claisen–Schmidt condensation. This green protocol offered significant advantages, including remarkably short reaction times (10 min), high yields (74% - 95%) and the use of a mild base (piperidine) to prevent decomposition of the acid-sensitive scaffold. The structures of all new compounds were unequivocally confirmed by comprehensive spectroscopic analyses (IR, NMR and MS). Antioxidant evaluation using the DPPH assay revealed that the presence of a phenolic hydroxyl group is crucial for activity, with the vanillin-derived derivative **6g** exhibiting the most promising potency (~86.7% inhibition at 50 μM). The structure-activity relationship further indicated that the position of the hydroxyl group (e.g., *para* > *ortho* due to intramolecular hydrogen bonding) significantly influences the radical scavenging efficacy.

These findings primarily highlight microwave irradiation as a rapid and efficient strategy for constructing this privileged scaffold and provide preliminary *in vitro* evidence for the antioxidant potential of select derivatives. However, it is important to note that this study is limited to a single antioxidant assay (DPPH) and further pharmacological validation is required. Future work will focus on obtaining

crystallographic confirmation of the proposed intramolecular hydrogen bonding, determining IC_{50} values, exploring additional antioxidant assays (e.g., ABTS, FRAP) and evaluating the most active compounds in cell-based models of oxidative stress.

Acknowledgements

The authors would like to thank their colleagues and laboratory staff for their valuable assistance and discussions during the course of this work.

Declaration of Generative AI in Scientific Writing

The authors declare that generative AI tools were used solely to improve the readability and language of the manuscript. These tools were applied with full human oversight and the authors remain entirely responsible for the scientific content, analysis and conclusions. No AI tools were listed as authors or co-authors.

CRediT Author Statement

Ngoc Thanh Nguyen: Conceptualization, Methodology, Supervision, Writing - Original Draft, Project administration, Funding acquisition. **Thi Thu Giang Pham:** Investigation, Data curation, Formal analysis, Visualization, Writing - Review & Editing. **Thuy Van Ngo:** Validation, Writing - Review & Editing.

References

[1] A Gaspar, EMPJ Garrido, F Borges and JMPJ Garrido. Biological and medicinal properties of natural chromones and chromanones. *ACS Omega* 2024; **9(20)**, 21706-21726.

[2] LL Mao, Y Liu and JP Wan. An Update on the advances in chromone and the derivatives synthesis based on the key chromone annulation of o-hydroxyaryl enaminones. *Chinese Chemical Letters* 2024; **36(7)**, 110784.

[3] M Lucas, M Freitas, AMS Silva, E Fernandes and D Ribeiro. Styrylchromones: Biological activities and structure-activity relationship. *Oxidative Medicine and Cellular Longevity* 2021; **2021**, 2804521.

[4] RS Ipe, S Kumar, F Benny, J Jayan, A Manoharan, ST Sudevan, G George, P Gahtori, H Kim and B Mathew. A concise review of the recent structural explorations of chromones as MAO-B inhibitors: Update from 2017 to 2023. *Pharmaceuticals* 2023; **16(9)**, 1310.

[5] A Sobha, A Ganapathy, S Mohan, N Madhusoodanan, AD Babysulochana, K Alaganandan and SB Somappa. Novel small molecule-based Acetylcholinesterase (AChE) inhibitors: From biological perspective to recent developments. *European Journal of Medicinal Chemistry Reports* 2024; **12**, 100237.

[6] M Asim, MK Jastrzębski and AA Kaczor. Dual inhibitors of acetylcholinesterase and monoamine Oxidase-B for the treatment of Alzheimer's disease. *Molecules* 2025; **30(14)**, 2975.

[7] KM Khan, A Ahmad, N Ambreen, A Amyn, S Perveen, SA Khan and MI Choudhary. Design, synthesis and biological evaluation of pyrazole derivatives as anticancer agents. *Letters in Drug Design & Discovery* 2009; **6**, 363-373.

[8] GP Ellis. *Chromenes, Chromanones, and Chromones: The chemistry of heterocyclic compounds*. John Wiley & Sons, New York, 1977, p. 495-555.

[9] W Baker. Molecular rearrangement of some o-acyloxyacetophenones and the mechanism of the production of 3-acylchromones. *Journal of the Chemical Society* 1933; **1933**, 1381-1389.

[10] S Tummanapalli, SK Punna, KC Gulipalli, S Endoori, S Bodige, AK Pommidi, S Medaboina, S Choppadandi, R Boya, VK Ganapathi, DY Mamindla, R Konakalla, GK Bodala, MR Bakangari, SD Kottam, D Jarikote, T Potewar and M Valluri. One-Pot Synthesis of Chromone-2-carboxylate Scaffold: An important pharmacophore with diverse biological properties. *The Journal of Organic Chemistry* 2023; **88(13)**, 8387-8399.

[11] M Wang, L Cheng, J Ma, W Lu and J Wang. Base-Promoted difunctionalization of alkynes: One-Pot synthesis of polysubstituted chromones. *European Journal of Organic Chemistry* 2023; **26(32)**, e202300456.

[12] MK Sharma, B Tiwaria and N Hussain. Pd-Catalyzed stereoselective synthesis of chromone C-Glycosides. *Chemical Communications* 2024; **60(36)**, 4838-4841.

[13] Y Chen, T Deng, S Zhu, F Yin and H Zhu. Divergent synthesis of chromones and chromanones from diketones using an AgOTf/[Si]H system by switching hydrosilanes. *Tetrahedron* 2024; **162**, 134087.

[14] X Wang, M Peng, Y Wang, S Song, Y Xu, L Chen and F Yu. Eco-Friendly and efficient synthesis of 2-Hydroxy-3-Hydrazono-Chromones through α,β-C(sp2)–H Bond difunctionalization/chromone annulation reaction of O-Hydroxyaryl Enaminones, Water and Aryldiazonium Salts. *Molecules* 2025; **30(6)**, 1194.

[15] S Song, M Peng, Z Zhang, H Hu, Y Wei, SJ Yan, Y Wang and F Yu. Divergent synthesis of 2-Chromonyl-3-hydrazono-chromones and 2-Alkoxy-3-hydrazono-chromones through switchable annulation reactions of O-Hydroxyphenylenaminones with aryldiazonium salts. *Organic Letters* 2024; **26(23)**, 4980-4985.

[16] G Tiwari, A Khanna, VK Mishra and R Sagar. Recent developments on microwave-assisted organic synthesis of Nitrogen- and Oxygen-Containing Preferred Heterocyclic Scaffolds. *RSC Advances* 2023; **13**, 32858-32892.

[17] Y Baqi and AH Ismail. Microwave-assisted synthesis of Near-Infrared chalcone dyes: A systematic approach. *ACS Omega* 2025; **10(7)**, 7317-7326.

[18] D Dotta, M Gastaldi, A Fin, N Barbero, C Barolo, F Cardano, F Rossi, F Brunelli, G Viscardi, GC Tron and P Quagliotto. Chalcone synthesis by Green Claisen–Schmidt reaction in cationic and nonionic micellar media. *The Journal of Organic Chemistry* 2025; **90(8)**, 2915-2926.

[19] A Mondal and C Mukhopadhyay. Solvent-Free microwave reactions towards significant organic transformations: A green approach. *Tetrahedron Green Chemistry* 2024; **4**, 100054.

[20] AA Shahat, P Cos, N Hermans, S Apers, TD Bruyne, L Pieters, DV Berghe and AJ Vlietinck. Anticomplement and antioxidant activities of new acetylated flavonoid glycosides from Centaurium spicatum. *Planta Medica* 2003; **69(12)**, 1153-1156.

[21] M Okawa, J Kinjo, T Nohara and M Ono. DPPH (1,1-diphenyl-2-picrylhydrazyl) radical scavenging activity of flavonoids obtained from some medicinal plants. *Biological and Pharmaceutical Bulletin* 2001; **24(10)**, 1202-1205.

[22] MT Nguyen, VV Nguyen, QT Tran, DC Nguyen and TD Dong. The synthesis of some *α,β*-unsaturated ketones from derivatives of axetyl cumarines. *Vietnam Journal of Chemistry* 2009; **47(1)**, 22-27.

[23] NT Nguyen. 2011, Synthesis and transformation of some of *α,β*-unsaturated ketones containing benzopyrone ring. Ph. D. Dissertation. Hanoi National University of Education, Hanoi, Vietnam.

[24] TN Nguyen, GTT Pham and VT Ngo. Synthesis of some *Bis*(arylidenes) containing heterocyclic chromones and *α*-pyronochromones. *Arkivoc* 2024; **2024(8)**, 202412244.

[25] VV Kouznetsov and LDVV Méndez. An update on the chemistry of 4H-Pyrans and 4H-Pyran-4-ones. *Current Organic Chemistry* 2020; **24(17)**, 1934-1973.

[26] NA Al-Masoudi and YA Al-Soud. Enamine-mediated catalysis in organic synthesis: Recent advances. *Journal of Chemical Research* 2021; **45(7-8)**, 562-571.

[27] D Díaz-Oviedo, MA García-Revilla and MA Vázquez. Microwave-assisted organic synthesis: A review of recent advancements and applications. *Current Opinion in Green and Sustainable Chemistry* 2023; **42**, 100822.

[28] D Tan, V Strukil, C Mottillo and T Friščić. Mechanochemical organic synthesis: A journey through time and space. *Nature Reviews Chemistry* 2023; **7**, 51-56.

[29] O Dhanya, P Navya, PVR Mumthas, MS Thasni and CKS Saleem. A review of microwave-assisted chalcone synthesis: Advancements over conventional methods and their pharmacological actions. *International Journal of Pharmaceutical Sciences Review and Research* 2025; **85(3)**, 158-165.

[30] FMA Soliman, AF Mohamed, M Mohamed, NTA Dawood and LI Sadik. Microwave-assisted synthesis of novel chalcone derivatives and study of some of their antimicrobial activities. *European Journal of Pharmaceutical and Medical Research* 2018; **5(9)**, 1-10.

[31] MR Ahmad, VG Sastry, N Bano and S Anwar. Synthesis of novel chalcone derivatives by conventional and microwave irradiation methods and their pharmacological activities. *Arabian Journal of Chemistry* 2016; **9**, S931-S935.

[32] A Rayar, MSI Veitía and C Ferroud. An efficient and selective microwave-assisted Claisen–Schmidt reaction for the synthesis of functionalized benzalacetones. *SpringerPlus* 2015; **4**, 221.

[33] KM Schaich, X Tian and J Xie. Hurdles and pitfalls in measuring antioxidant efficacy: A critical evaluation of ABTS, DPPH, and ORAC assays. *Journal of Functional Foods* 2015; **14**, 111-125.

[34] AM Pisoschi, A Pop, F Iordache, L Stanca, G Predoi and AI Serban. Oxidative stress mitigation by antioxidants - An overview on their chemistry and influences on health status. *European Journal of Medicinal Chemistry* 2021; **209**, 112891.

[35] CC Shang, Y Zhang, C Sun and L Wang. Tactfully improve the antioxidant activity of 2′-hydroxychalcone with the strategy of substituent, solvent and intramolecular hydrogen bond effects. *Journal of Molecular Liquids* 2022; **362**, 119748.

[36] IR Ilyasov, VL Beloborodov, IA Selivanova and RP Terekhov. ABTS/PP decolorization assay of antioxidant capacity reaction pathways. *International Journal of Molecular Sciences* 2020; **21(3)**, 1131.

[37] KM Schaich, X Tian and J Xie. Hurdles and pitfalls in measuring antioxidant efficacy: A critical evaluation of ABTS, DPPH and ORAC assays. *Journal of Functional Foods* 2015; **14**, 111-125.

[38] NB Sadeer, D Montesano, S Albrizio, G Zengin and MF Mahomoodally. The versatility of antioxidant assays in Food Science and Safety-Chemistry, applications, strengths and limitations. *Antioxidants* 2020; **9(8)**, 709.

Appendixes

Appendixes: Spectral Data

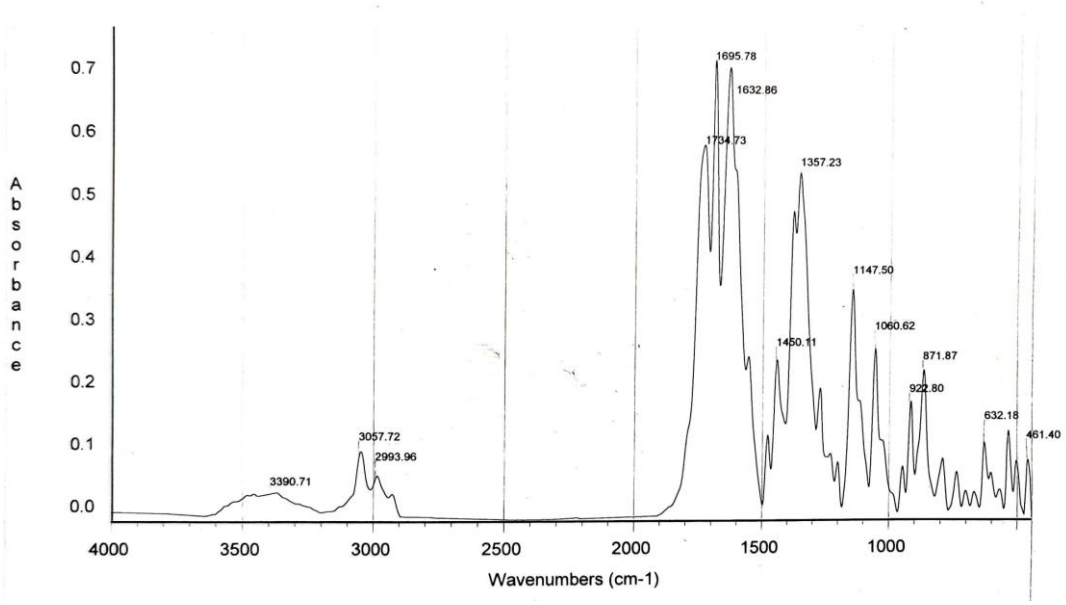

Figure 1 IR spectrum of compound 4.

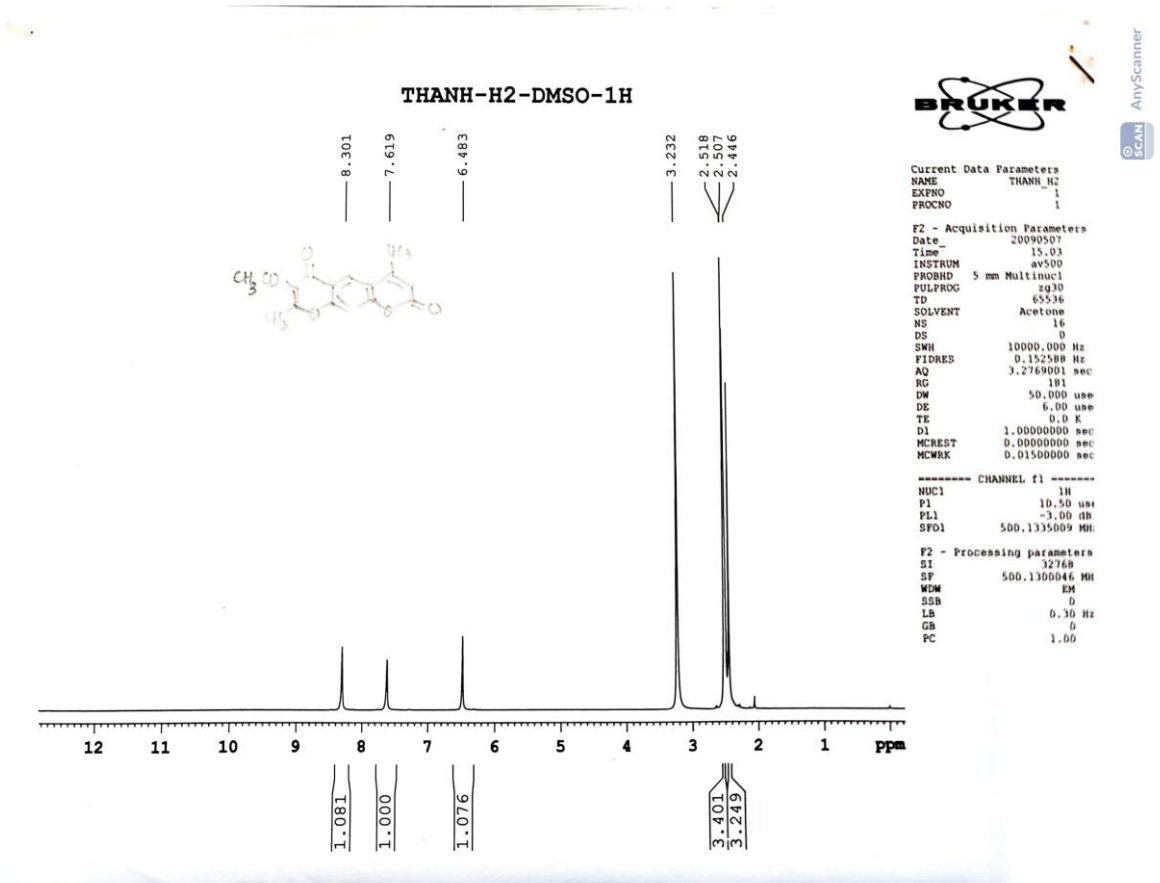

Figure 2 ^{1}H NMR spectrum of compound 4.

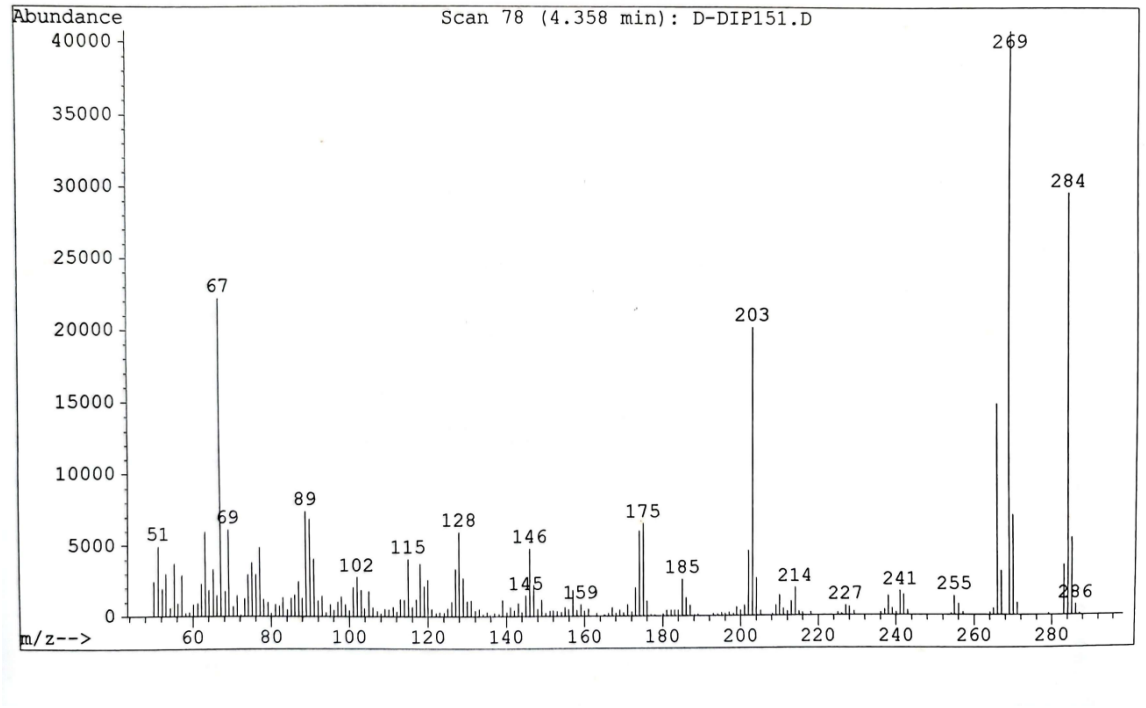

Figure 3 MS spectrum of compound 4.

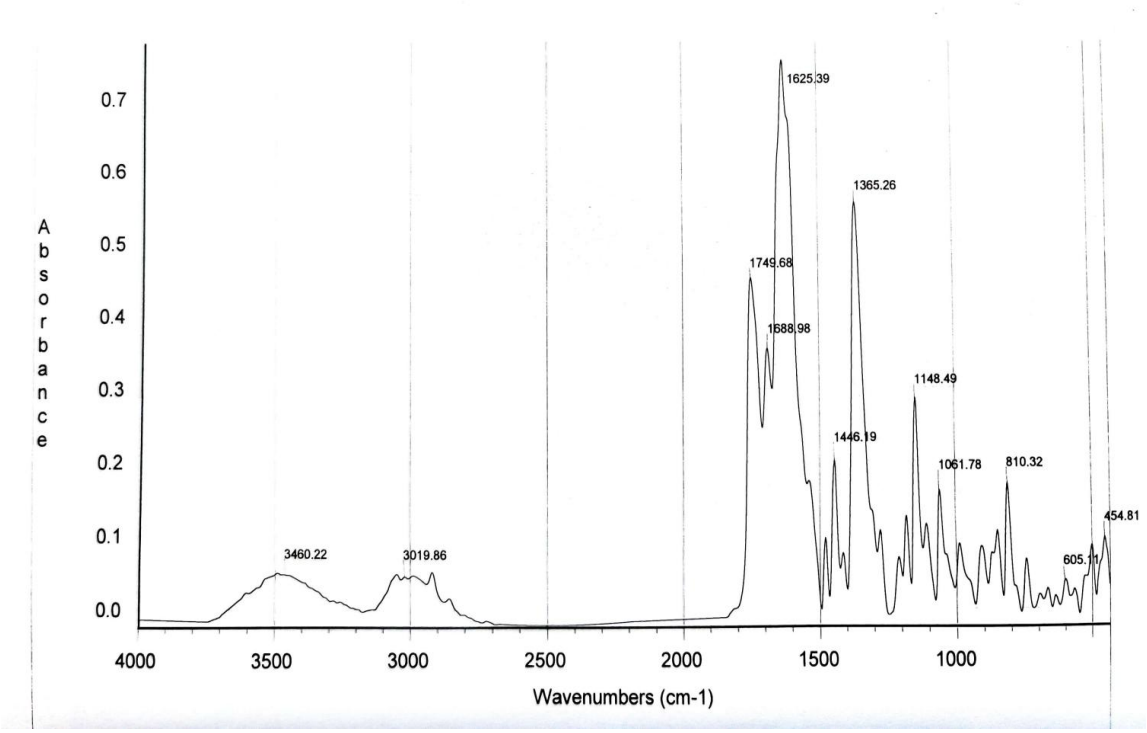

Figure 4 IR spectrum of compound 6a.

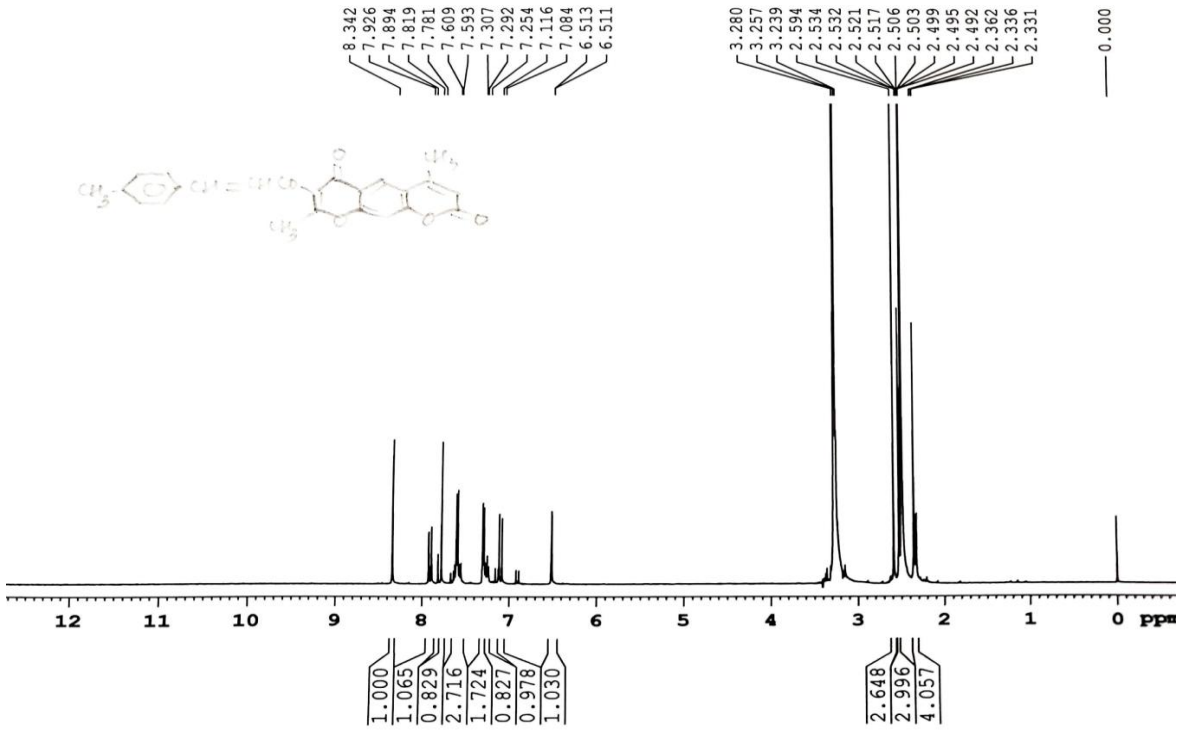

Figure 5 ^{1}H NMR spectrum of compound 6a.

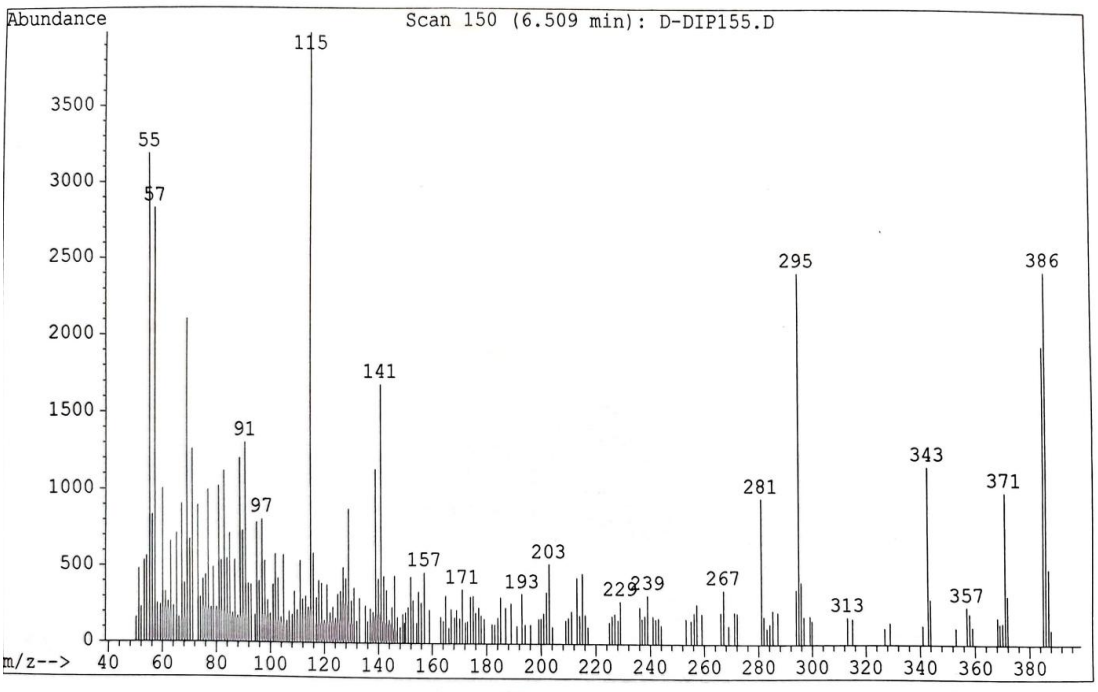

Figure 6 MS spectrum of compound 6a.

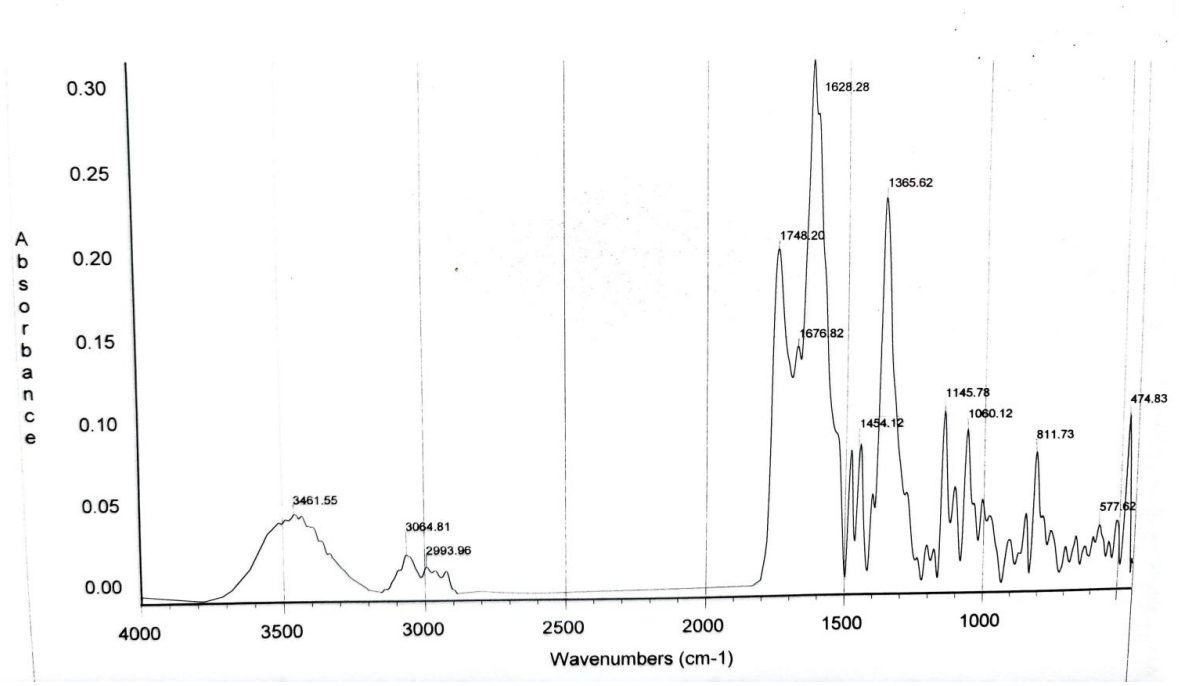

Figure 7 IR spectrum of compound 6b.

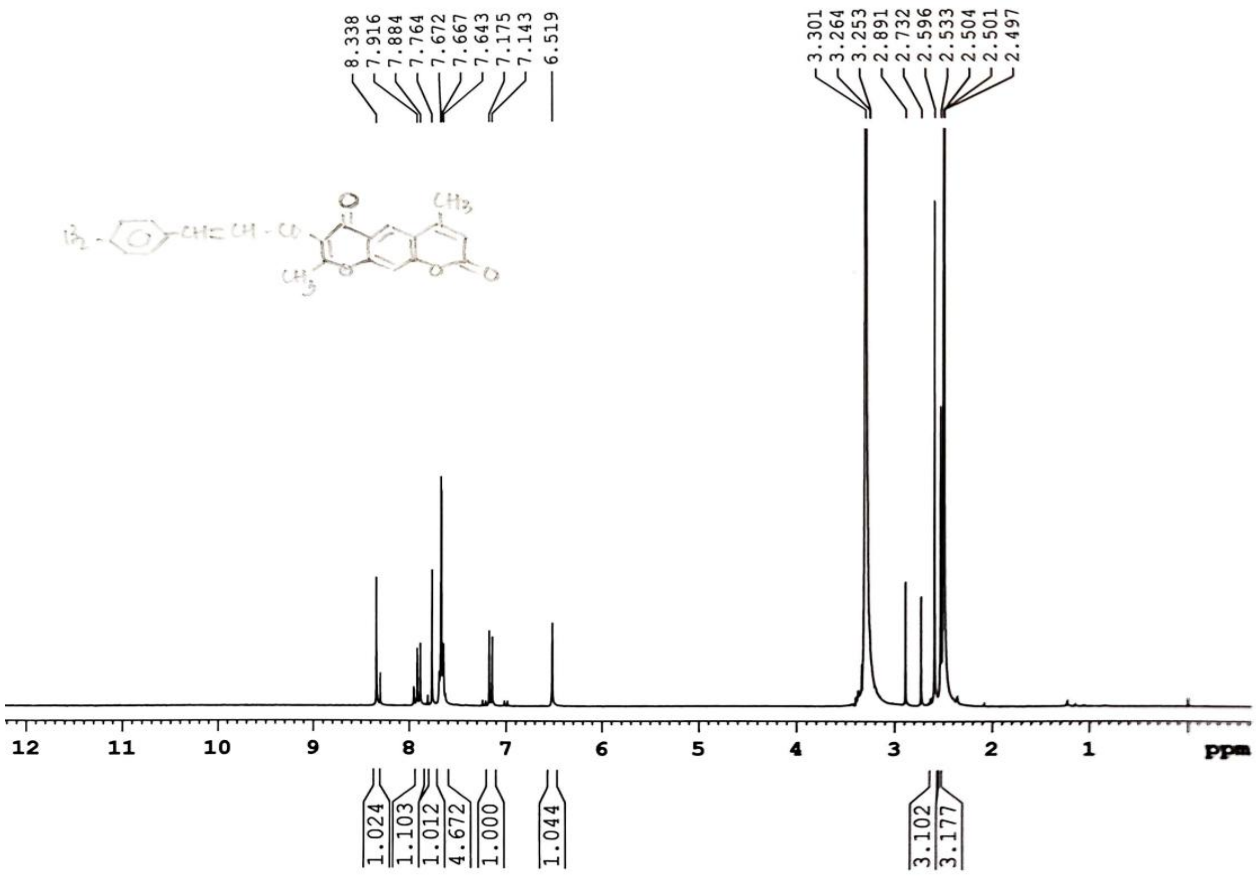

Figure 8 [1]H NMR spectrum of compound 6b.

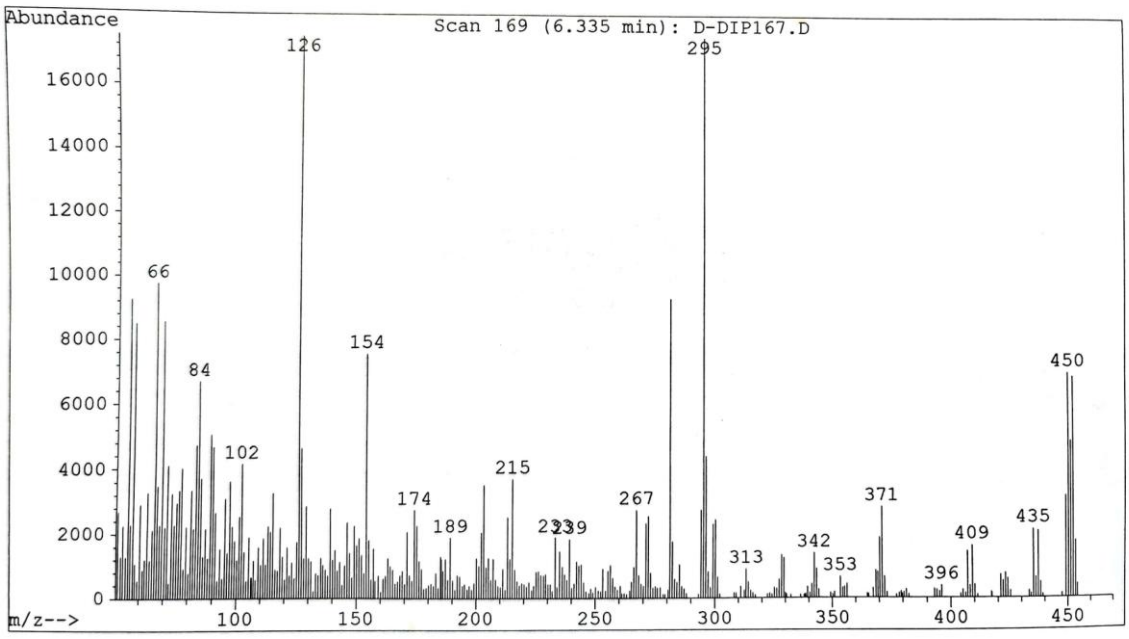

Figure 9 MS spectrum of compound 6b.

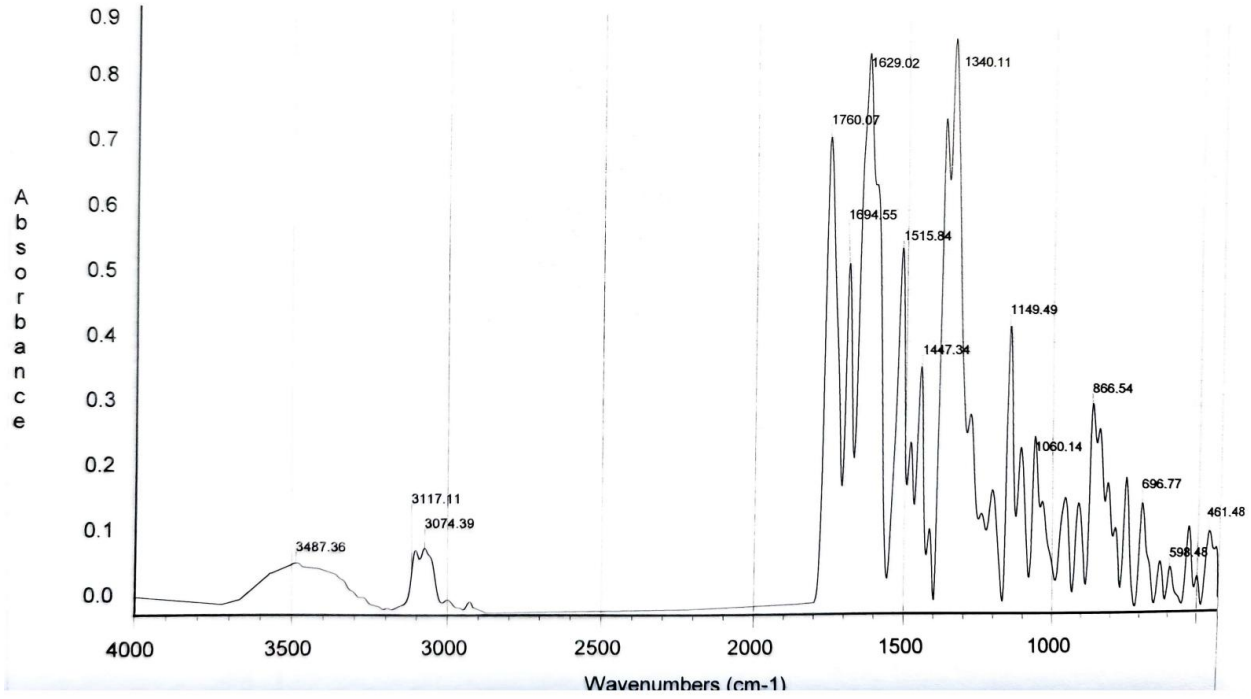

Figure 10 IR spectrum of compound 6c.

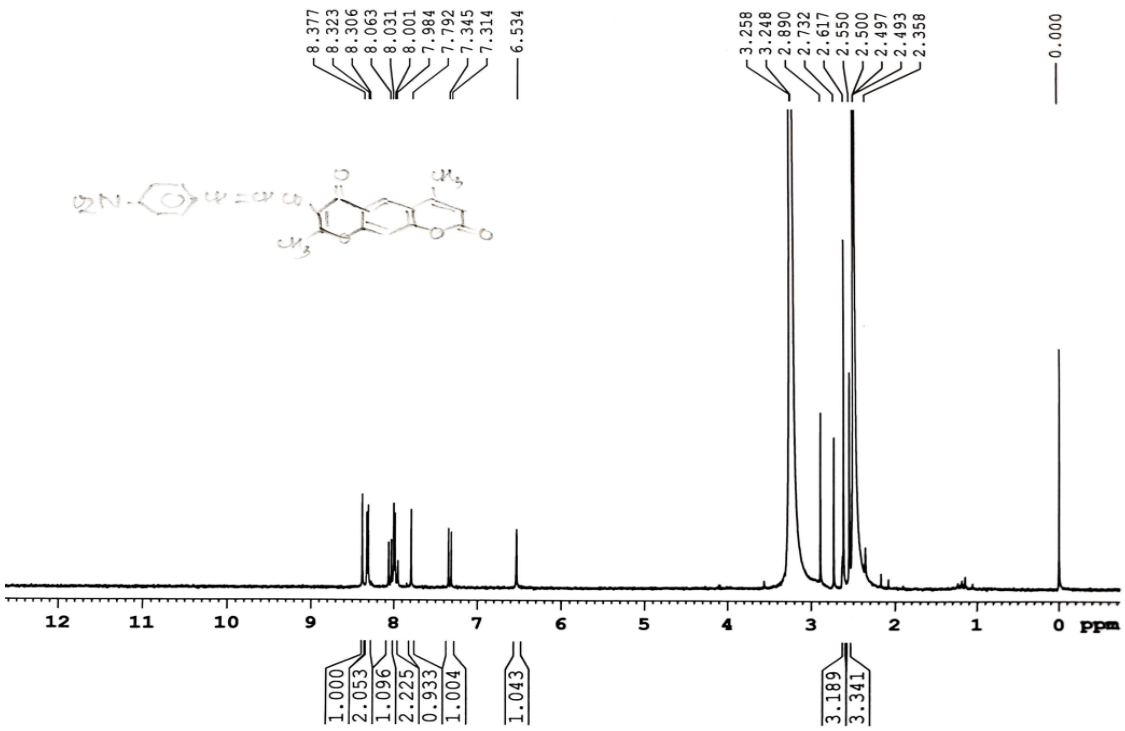

Figure 11 ^{1}H NMR spectrum of compound 6c.

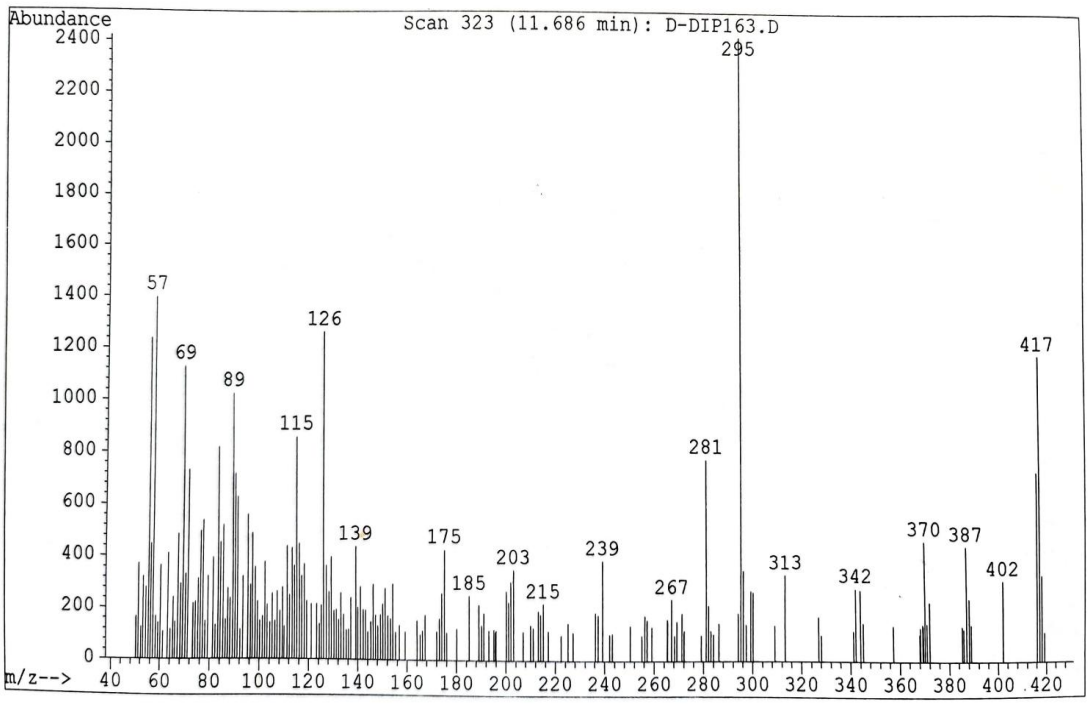

Figure 12 MS spectrum of compound 6c.

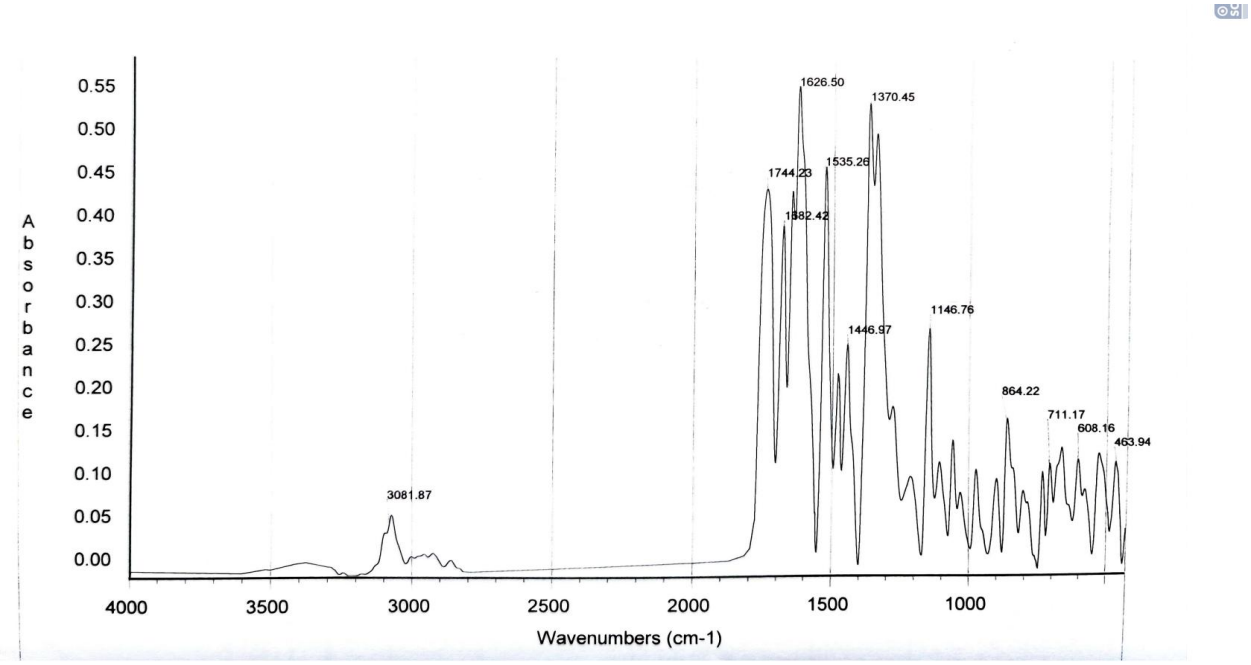

Figure 13 IR spectrum of compound 6d.

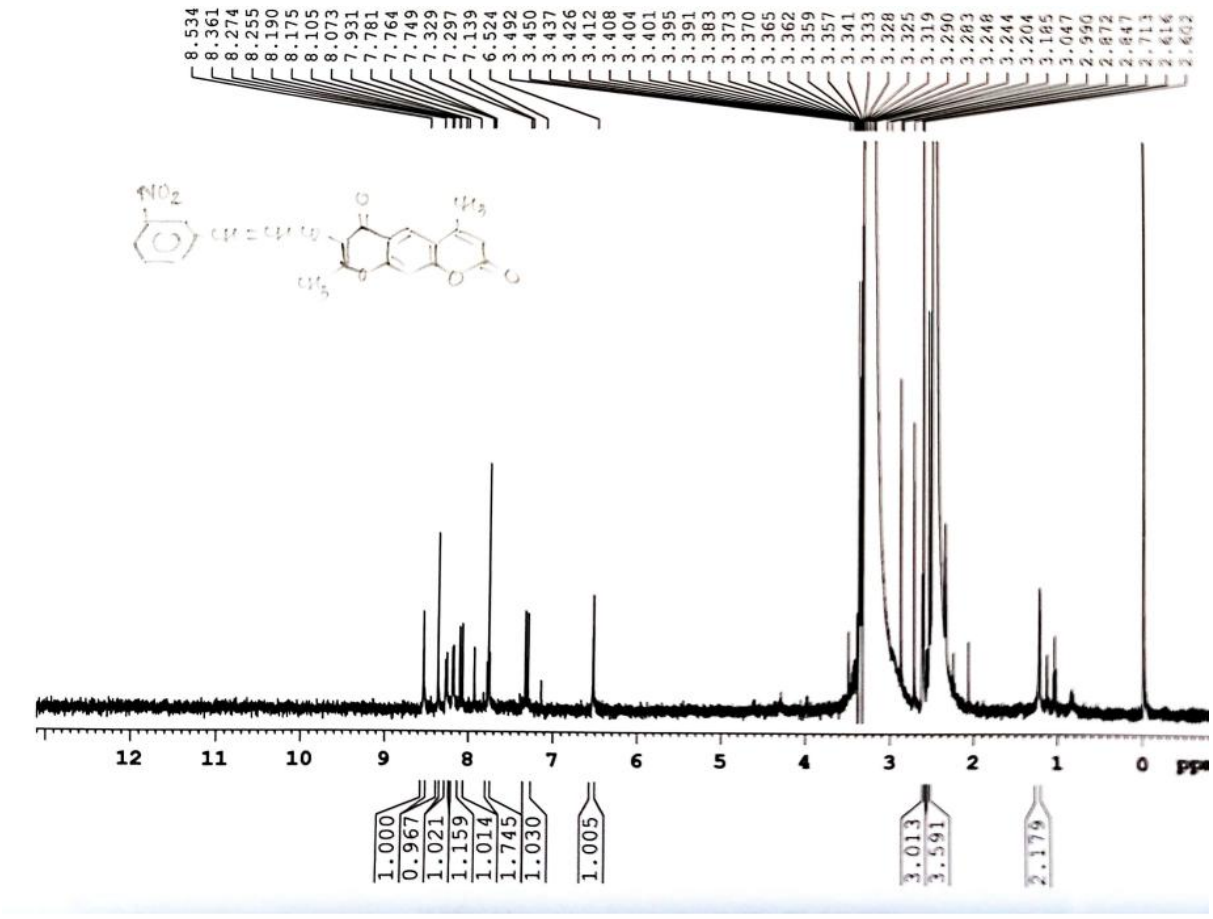

Figure 14 ^{1}H NMR spectrum of compound 6d.

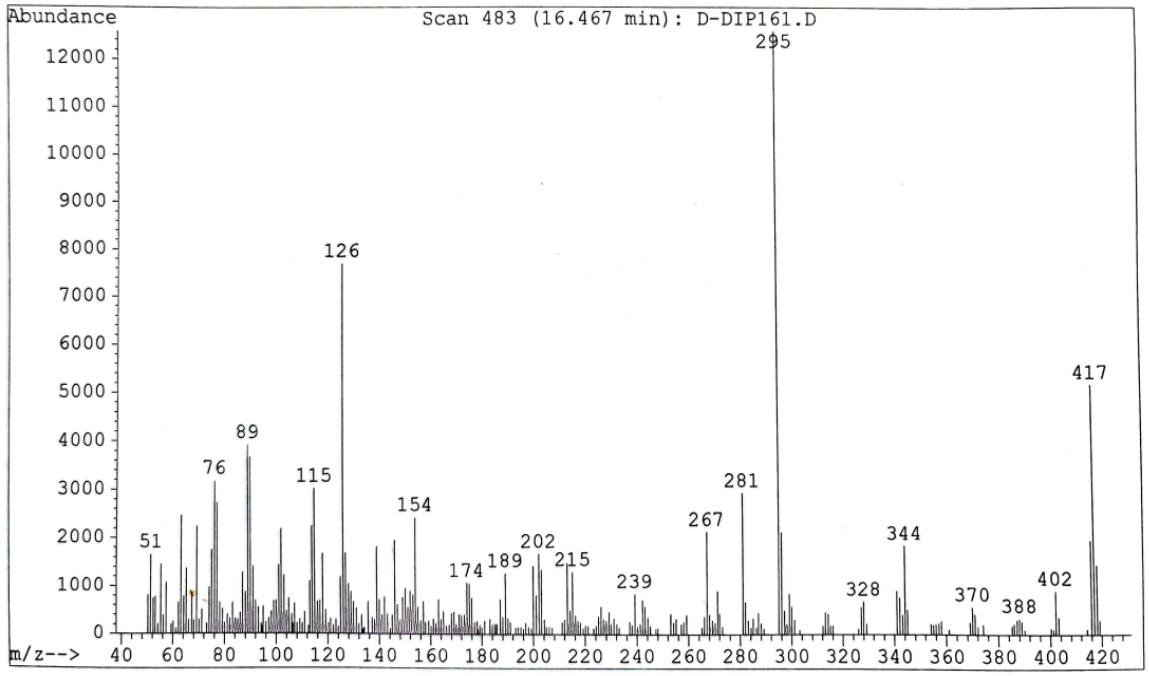

Figure 15 MS spectrum of compound 6d.

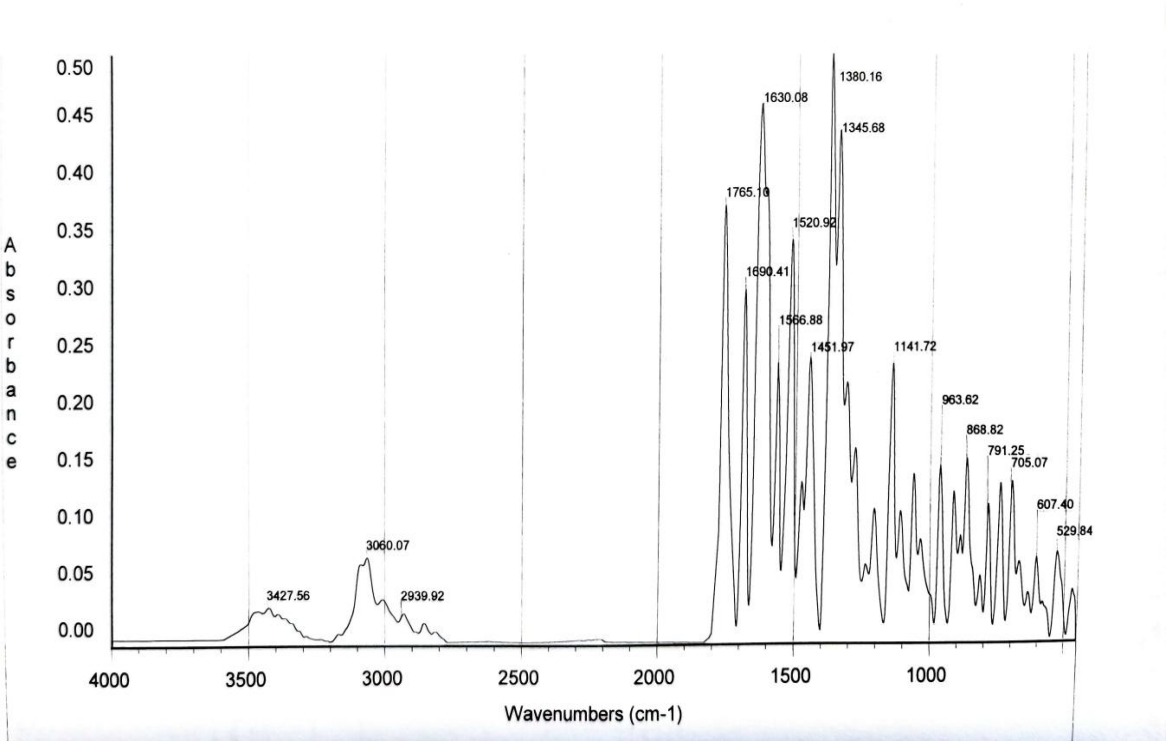

Figure 16 IR spectrum of compound 6e.

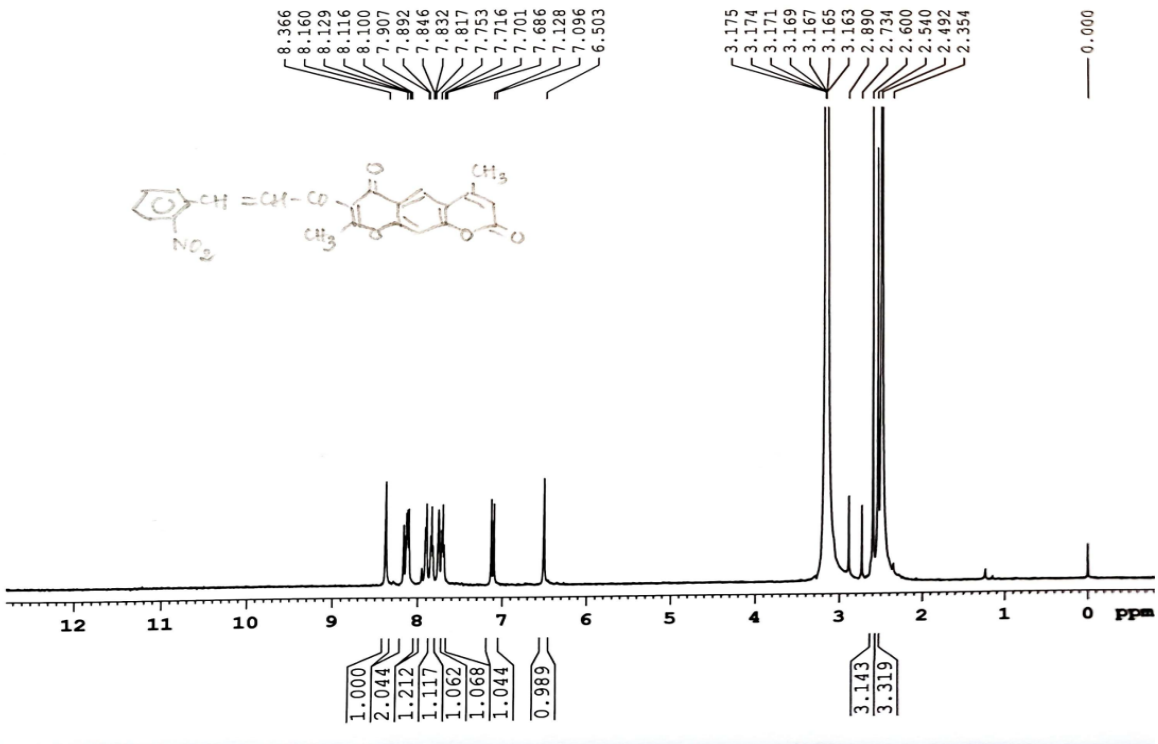

Figure 17 [1]H NMR spectrum of compound 6e.

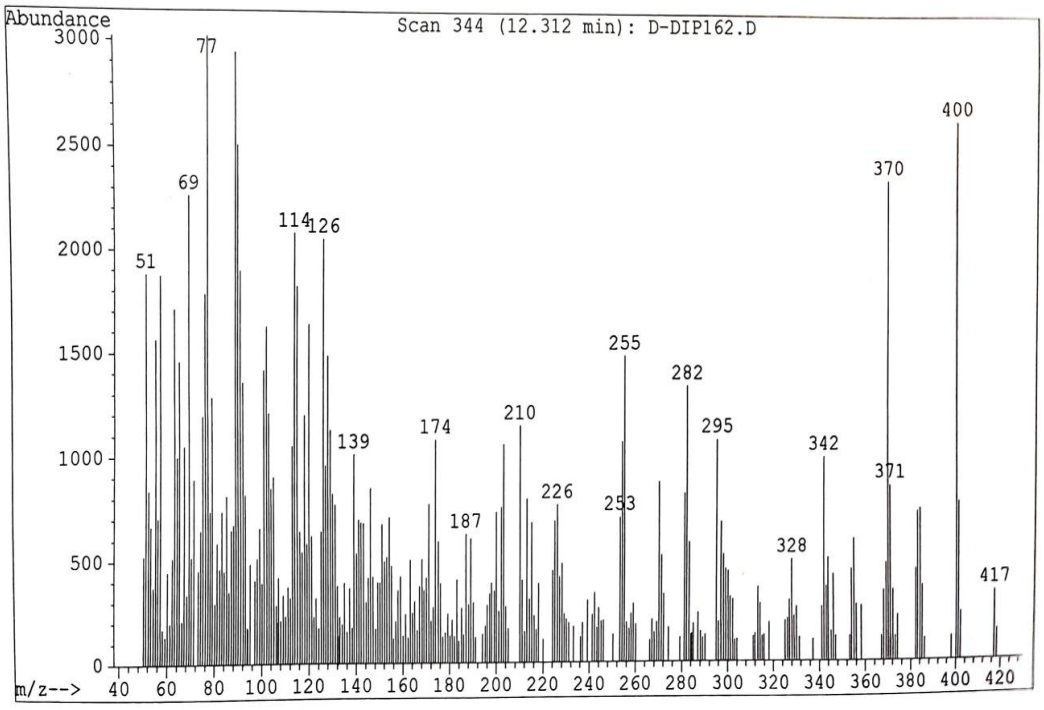

Figure 18 MS spectrum of compound 6e.

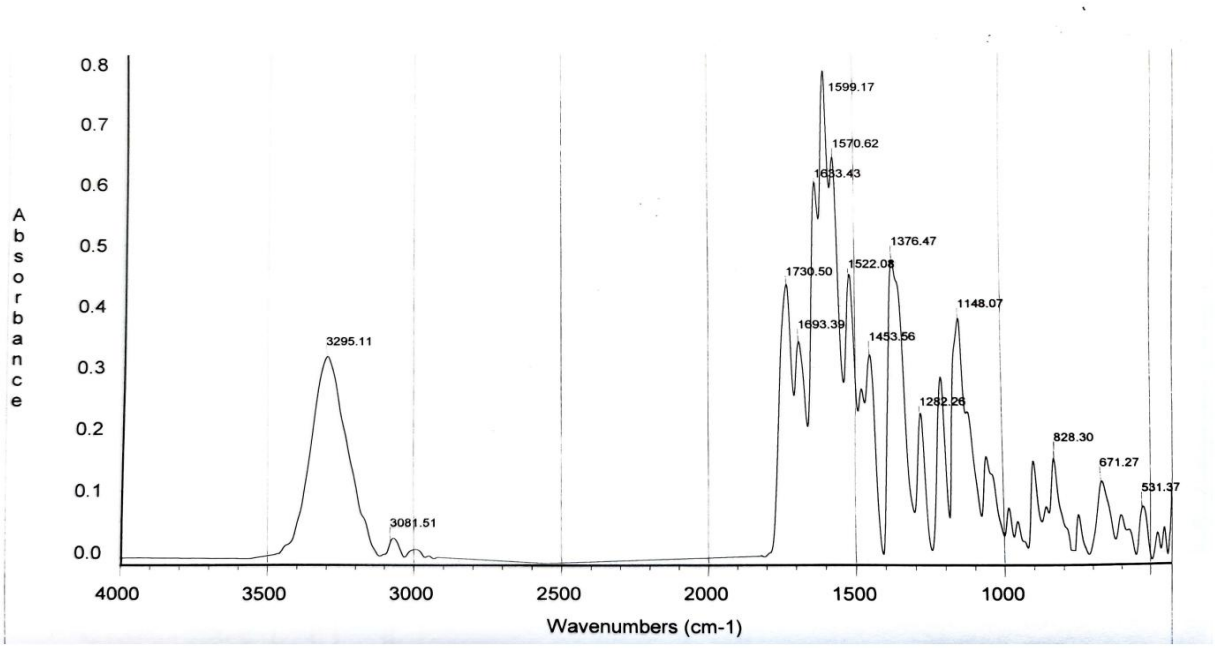

Figure 19 IR spectrum of compound 6f.

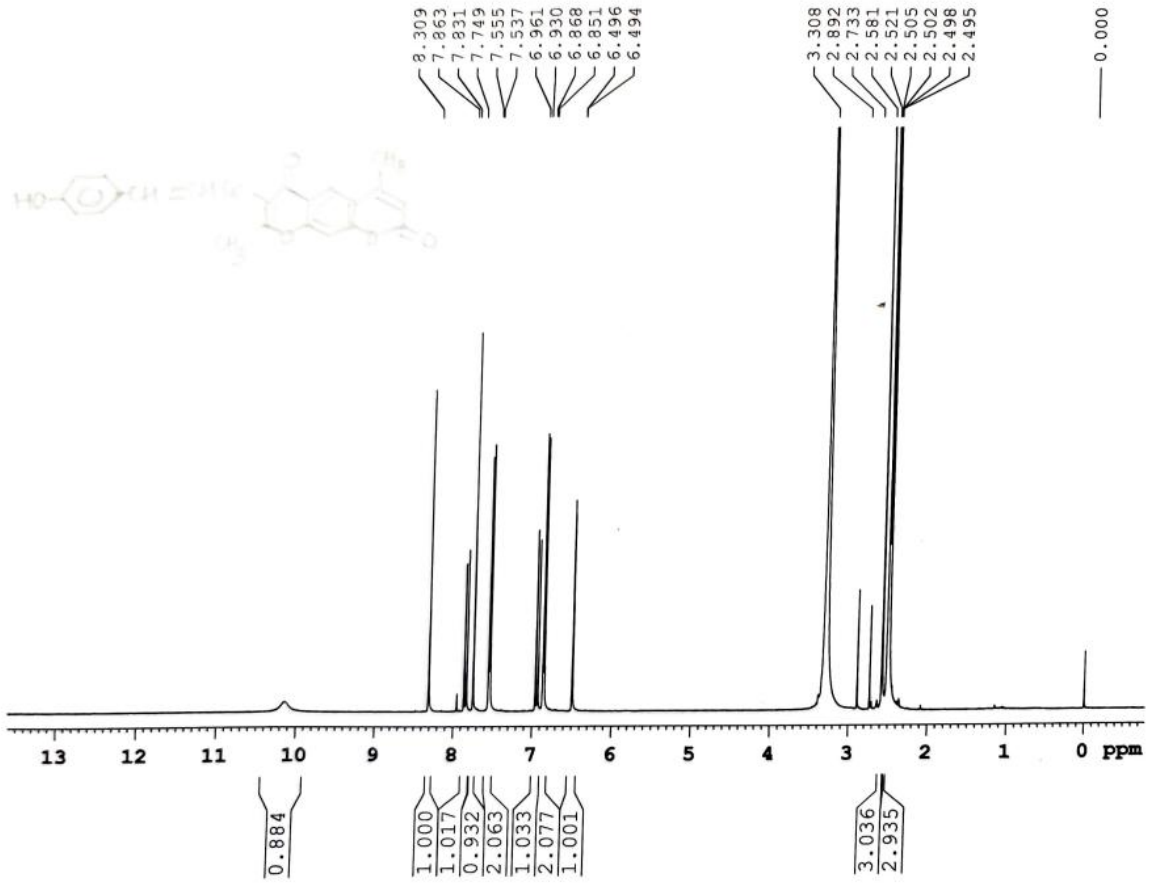

Figure 20 ^{1}H NMR spectrum of compound 6f.

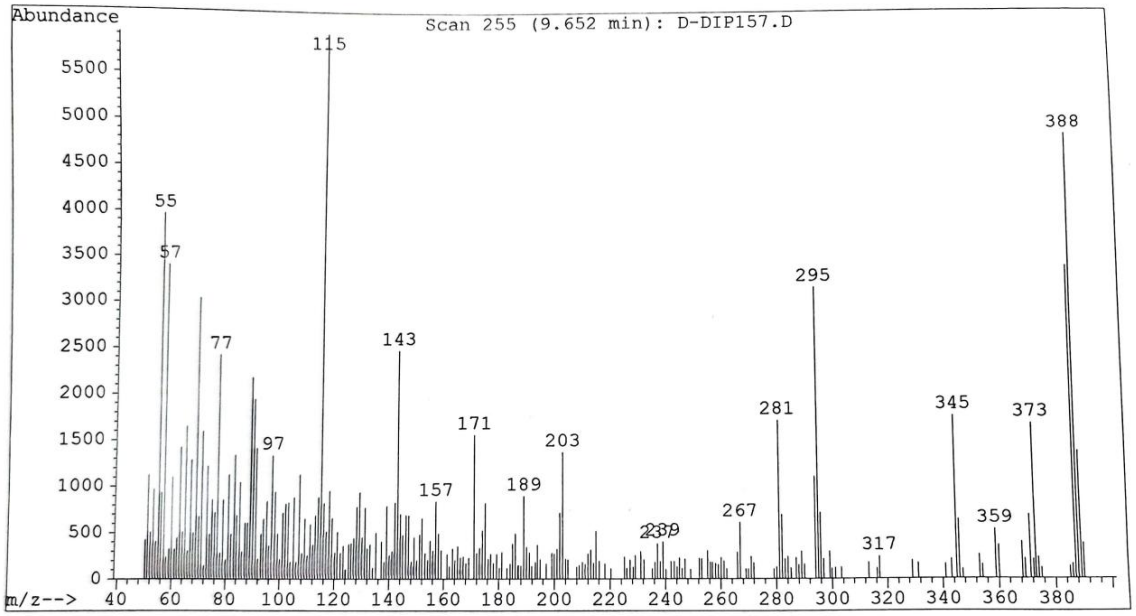

Figure 21 MS spectrum of compound 6f.

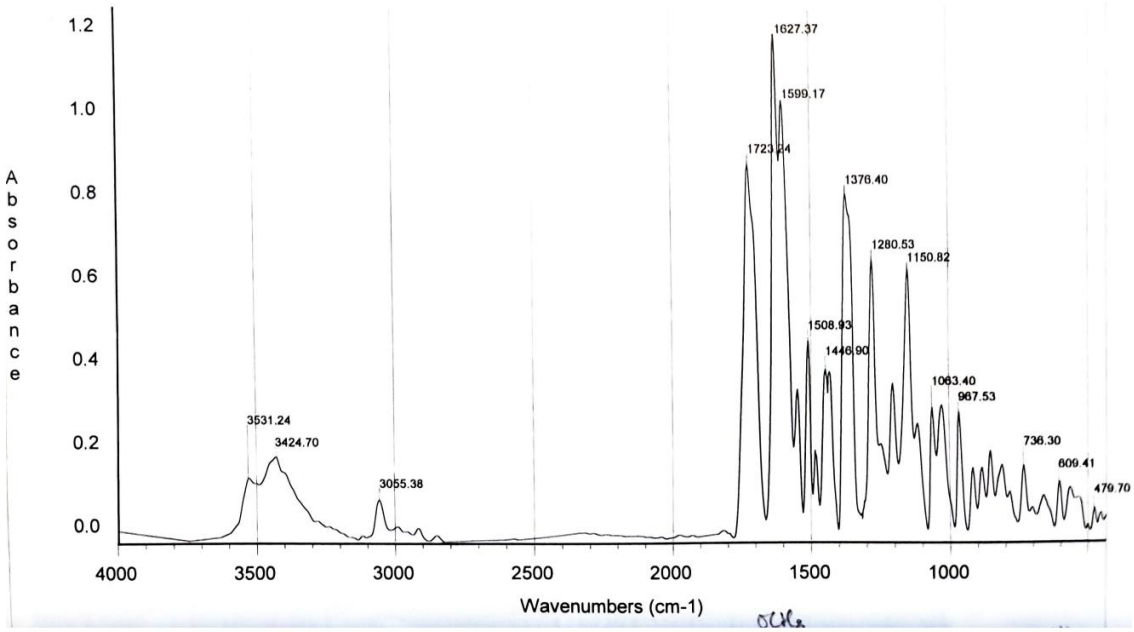

Figure 22 IR spectrum of compound 6g.

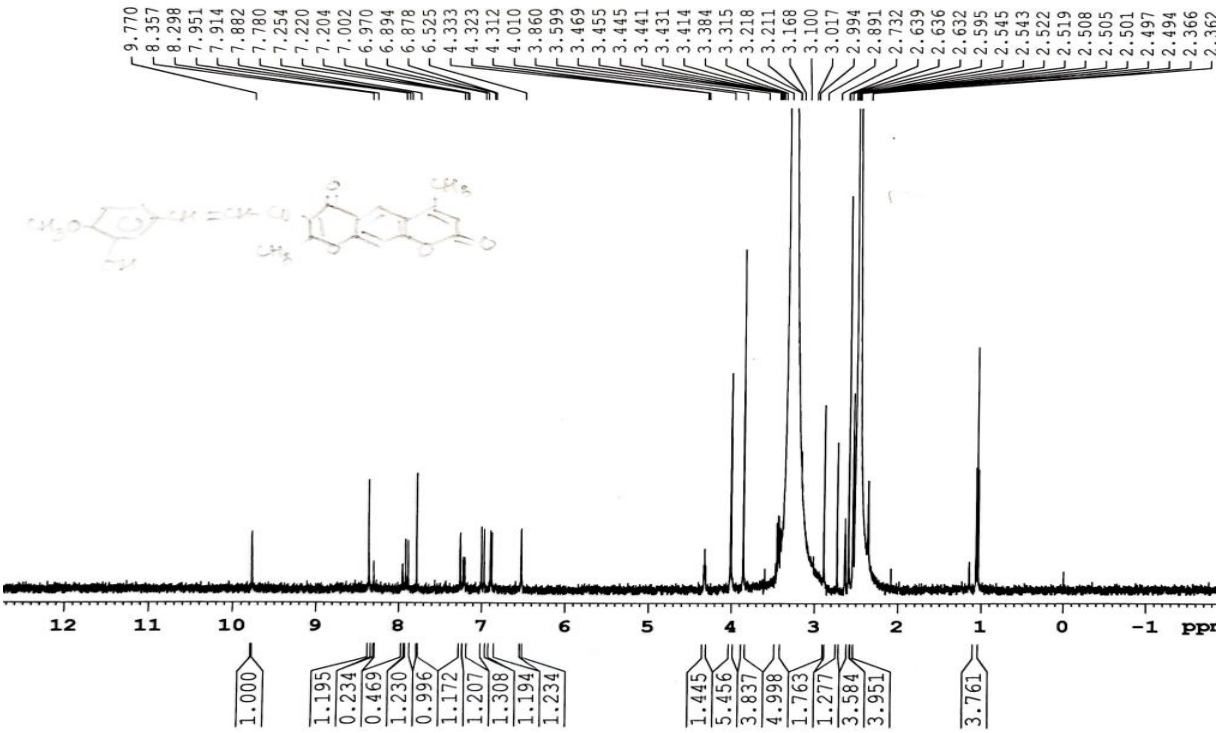

Figure 23 [1]H NMR spectrum of compound 6g.

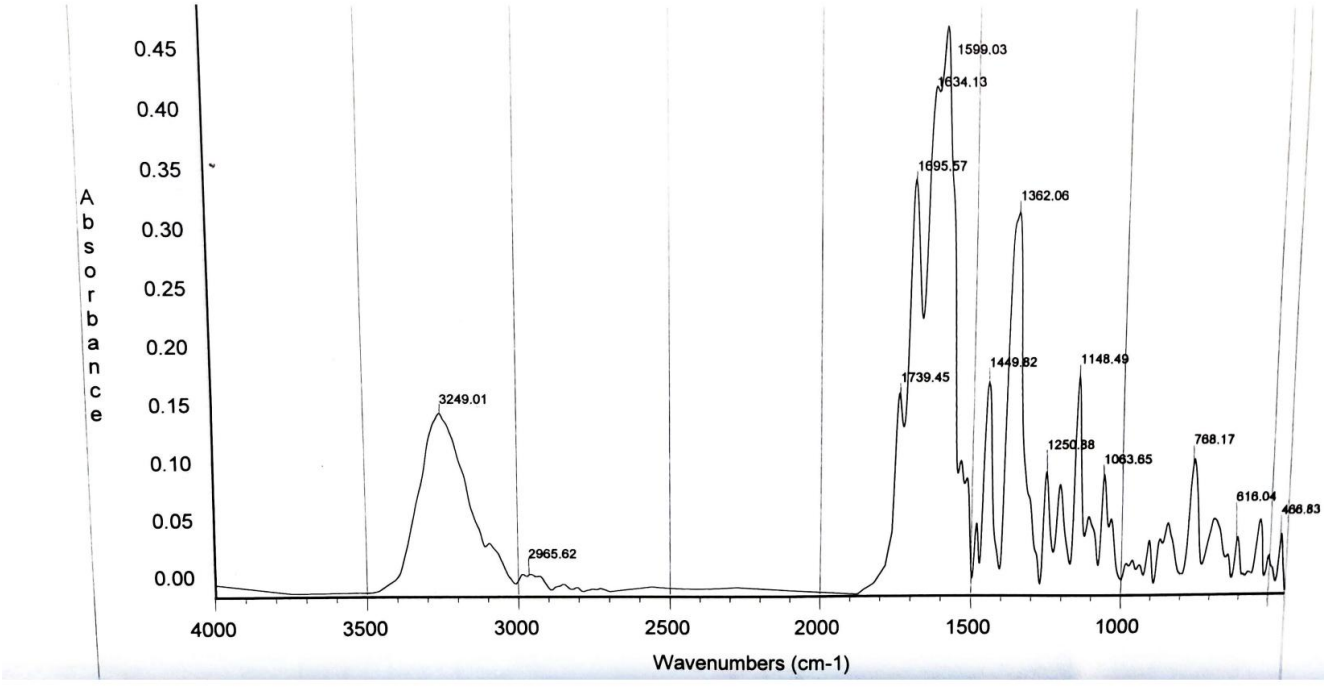

Figure 24 IR spectrum of compound 6h.

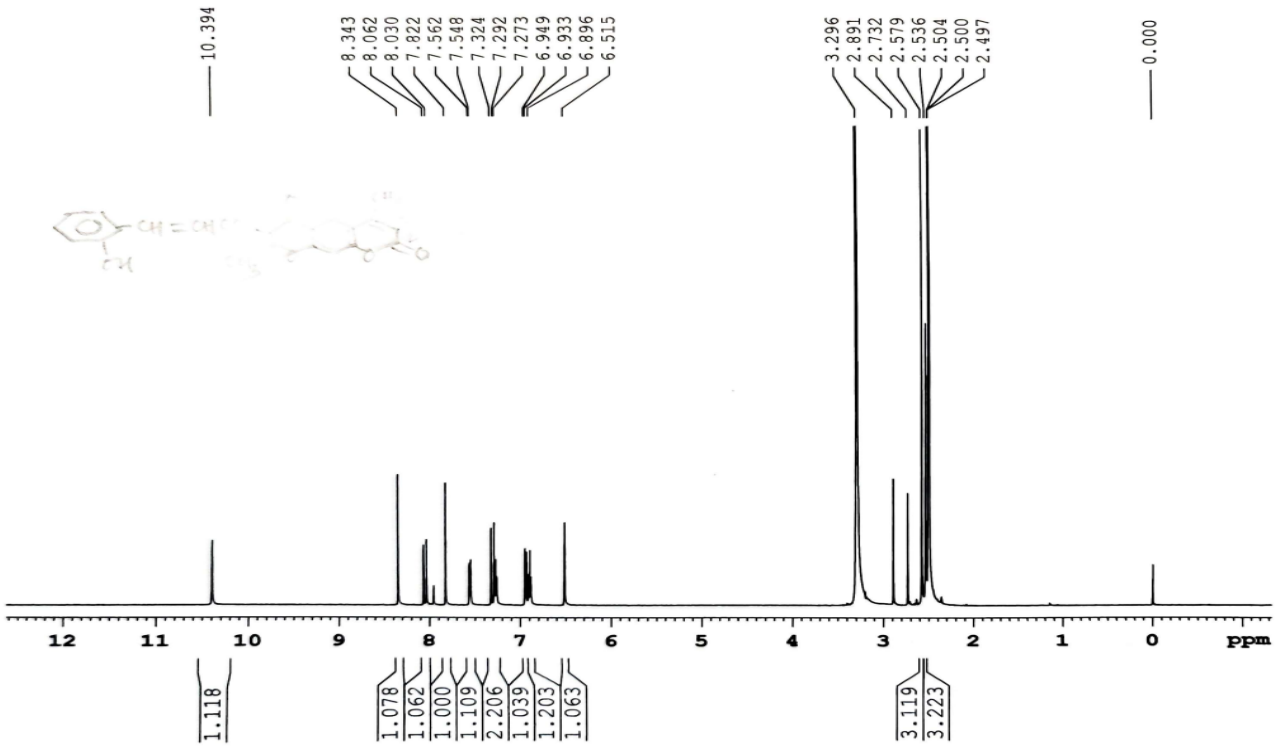

Figure 25 [1]H NMR spectrum of compound 6h.

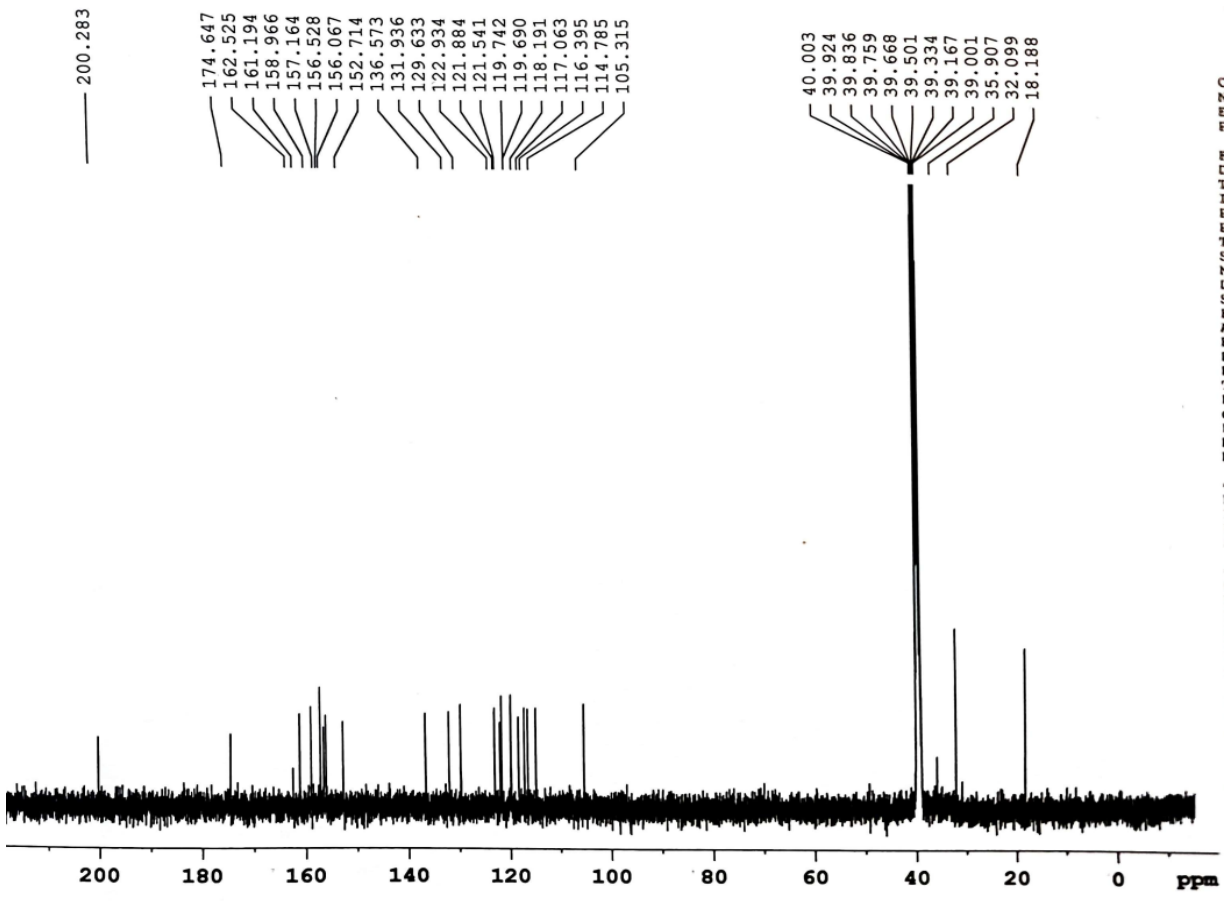

Figure 26 [13]C NMR spectrum of compound 6h.

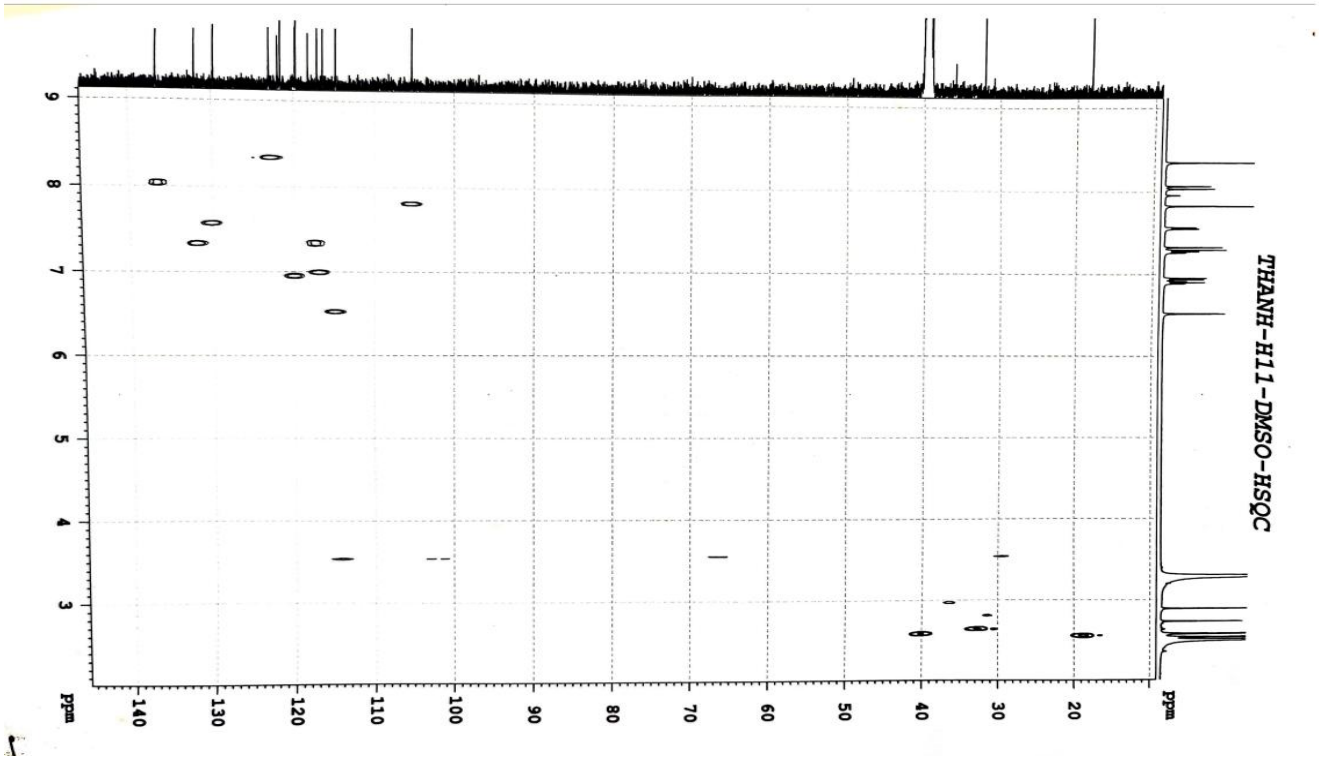

Figure 27 HSQC spectrum of compound 6h.

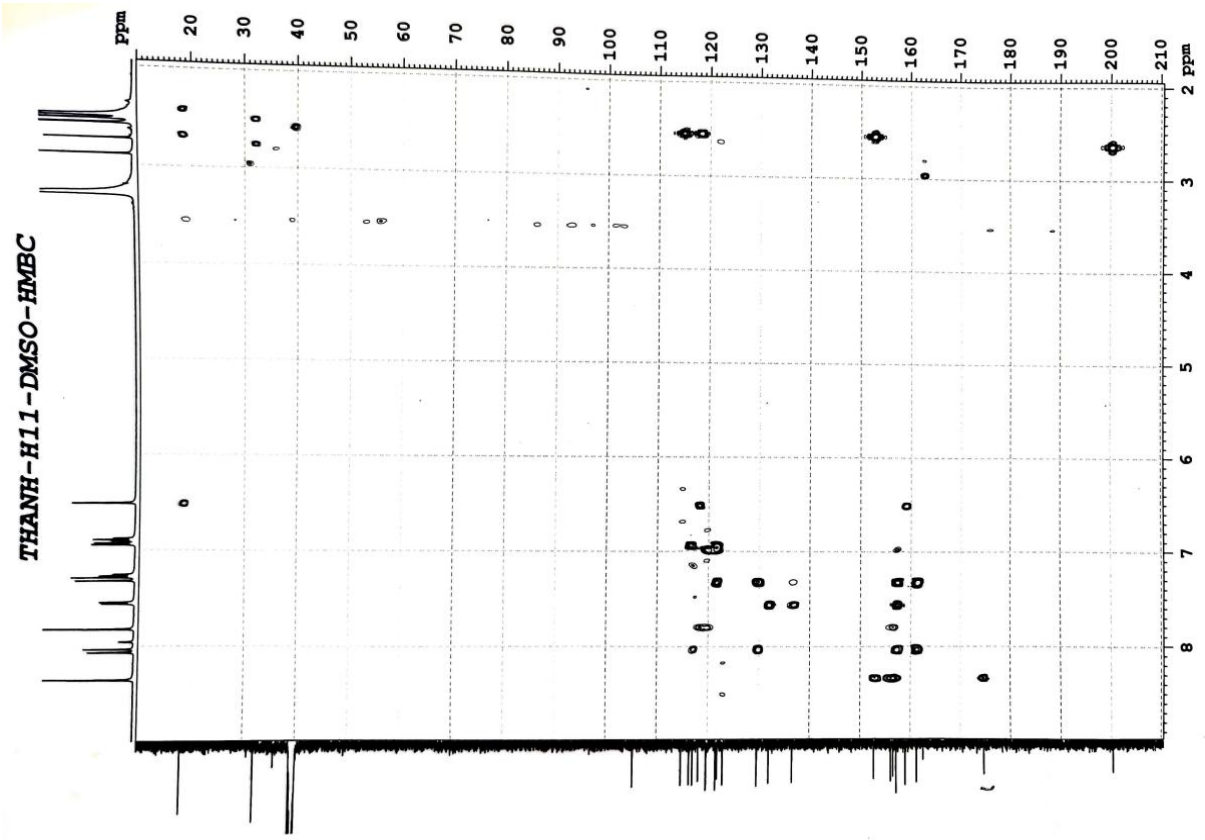

Figure 28 HMBC spectrum of compound 6h.

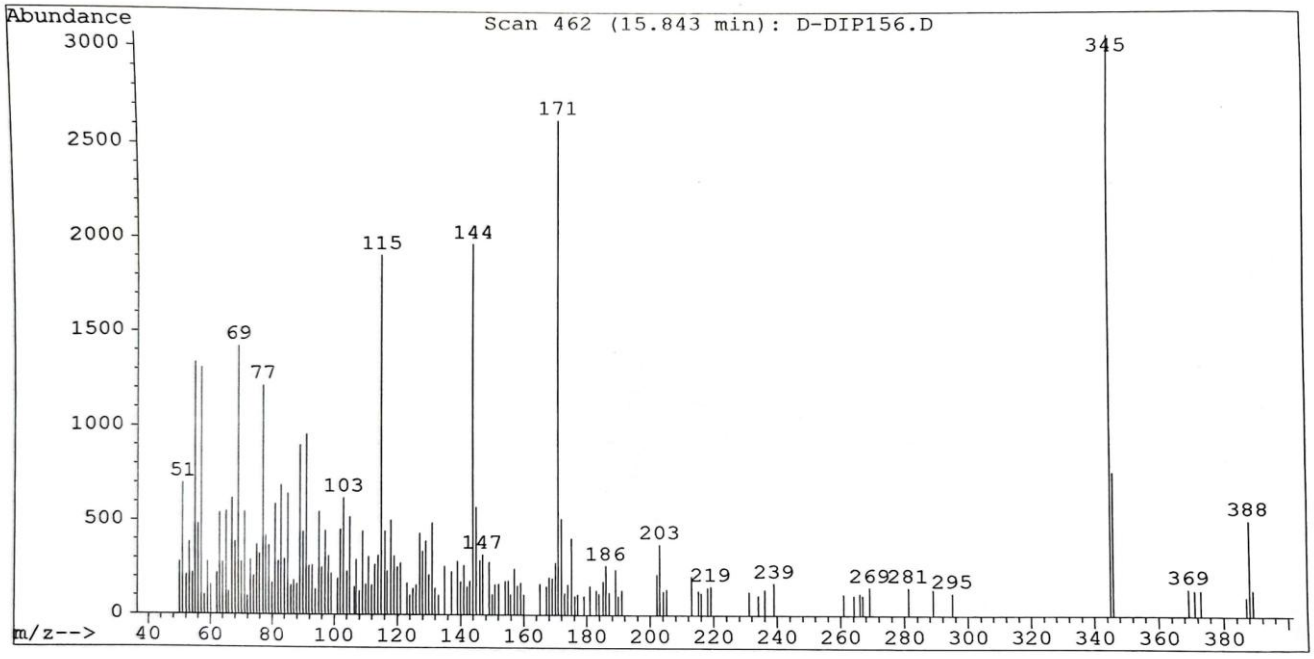

Figure 29 MS spectrum of compound 6h.

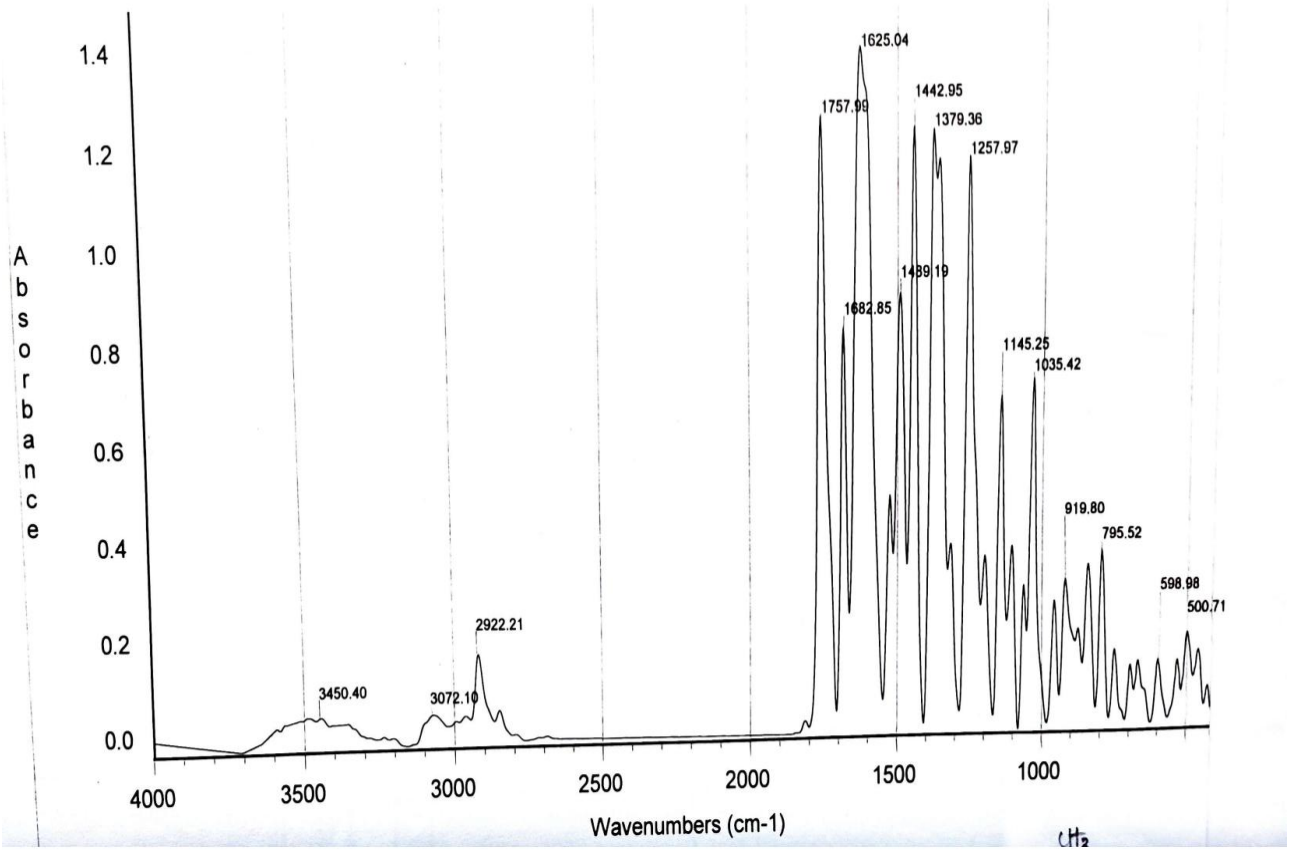

Figure 30 IR spectrum of compound 6i.

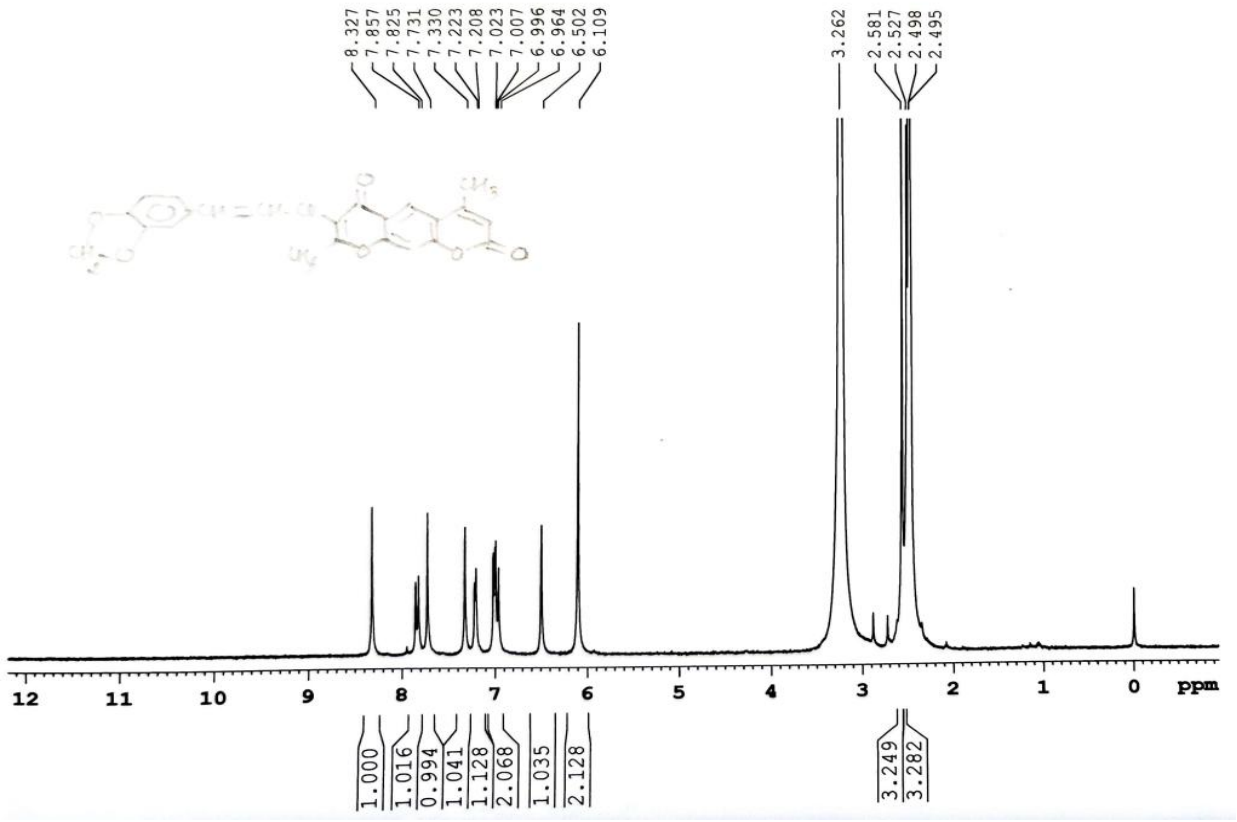

Figure 31 [1]H NMR spectrum of compound 6i.

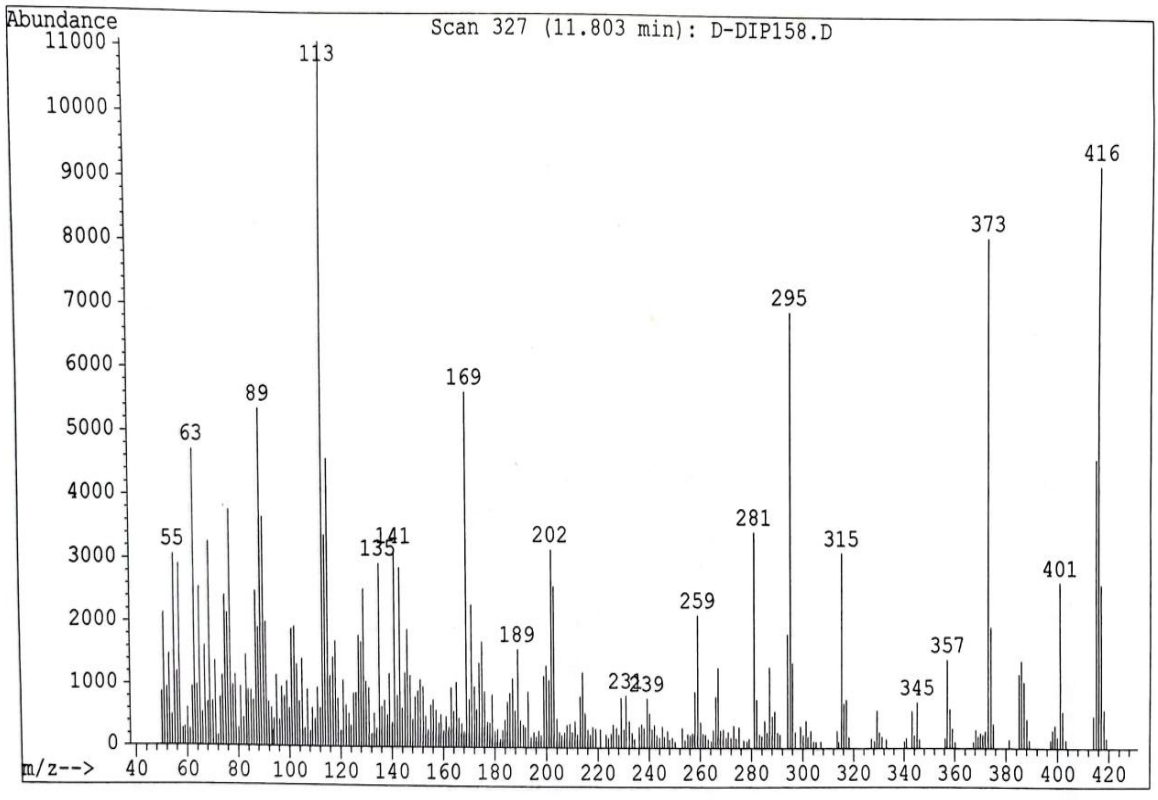

Figure 32 MS spectrum of compound 6i.

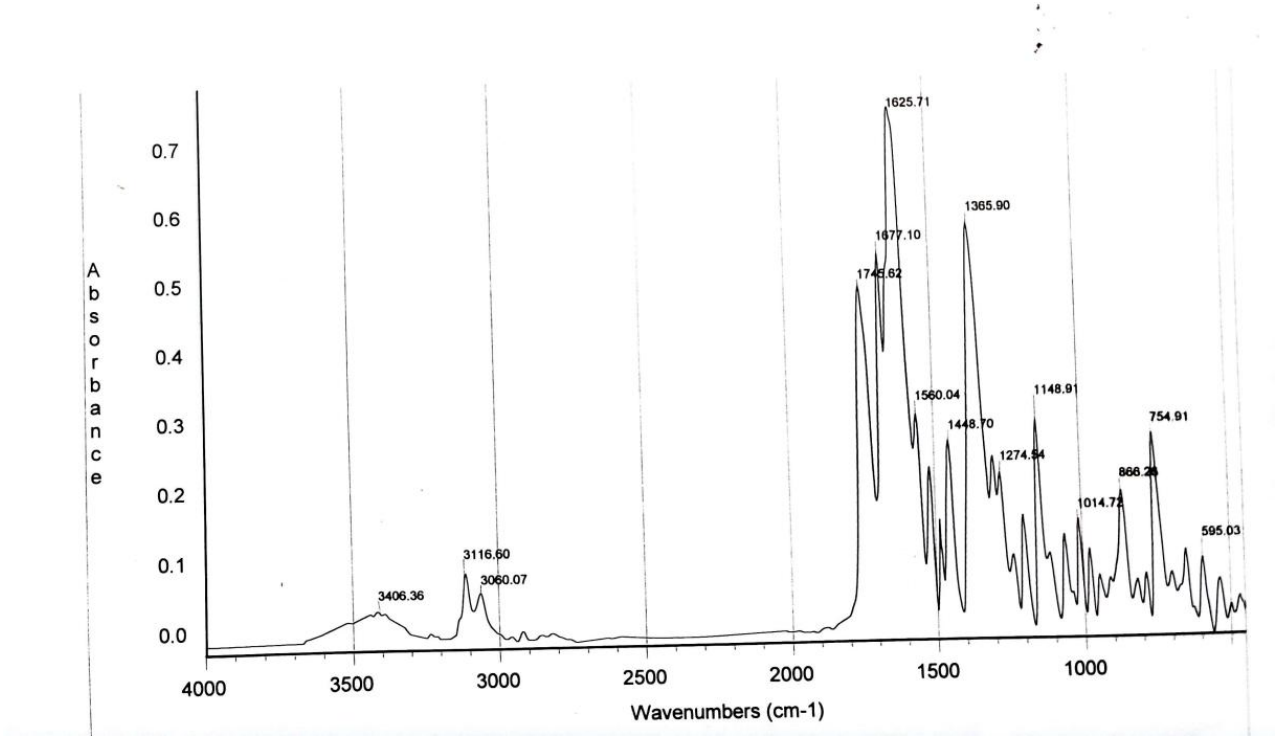

Figure 33 IR spectrum of compound 6j.

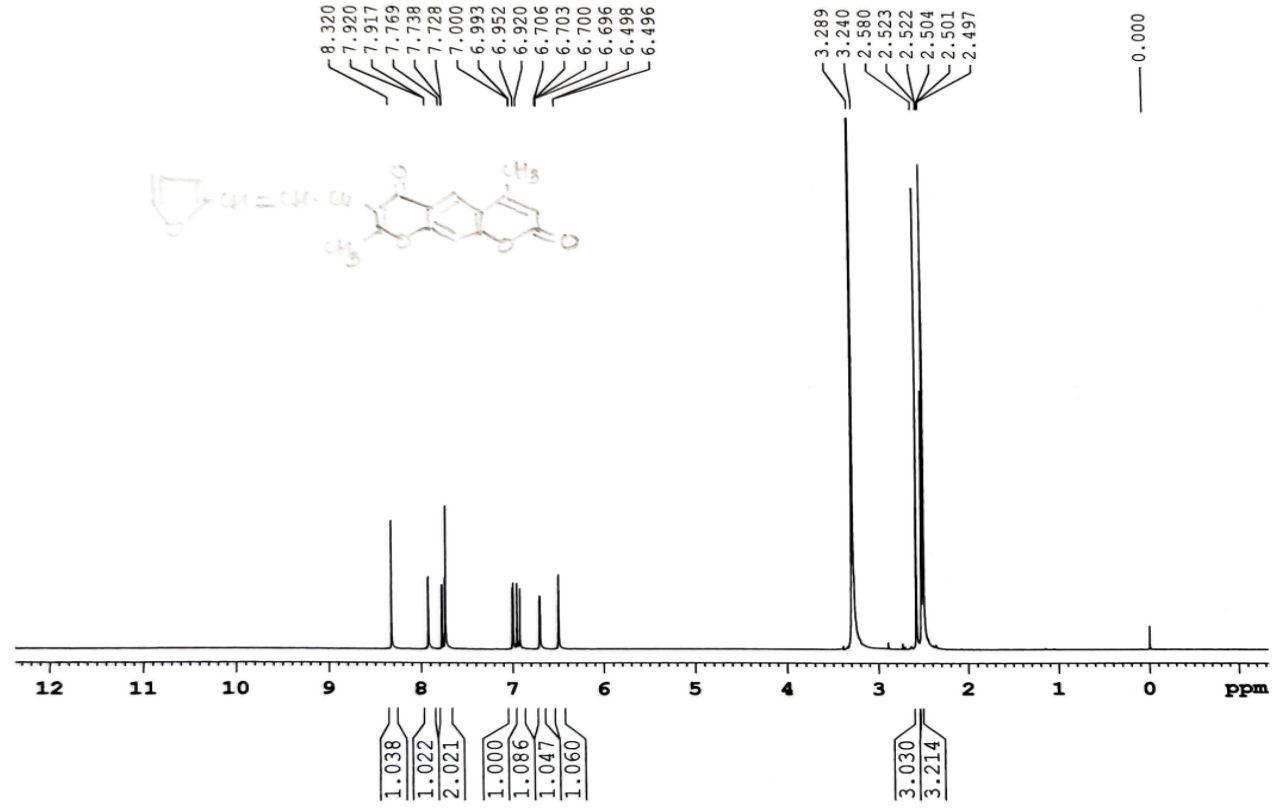

Figure 34 ^{1}H NMR spectrum of compound 6j.

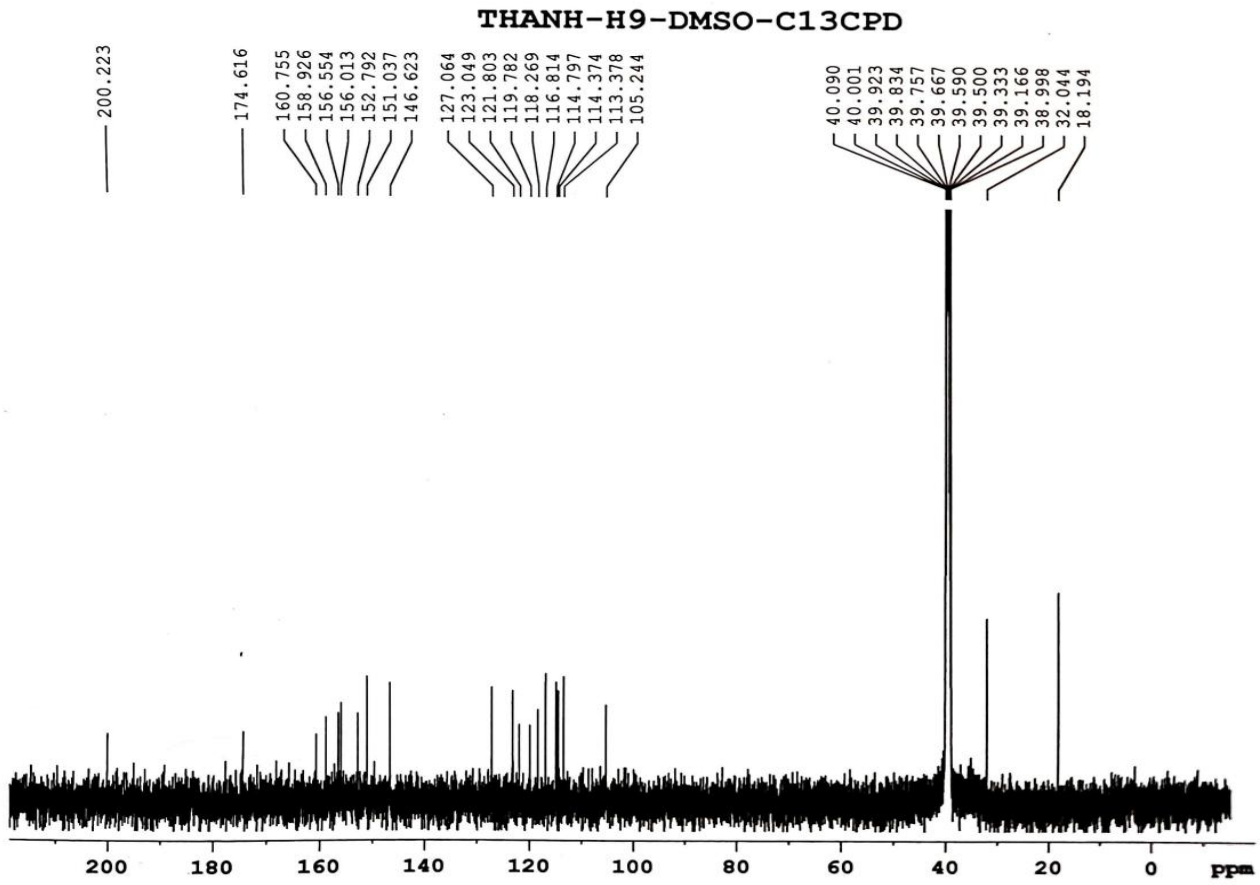

Figure 35 ^{13}C NMR spectrum of compound 6j.

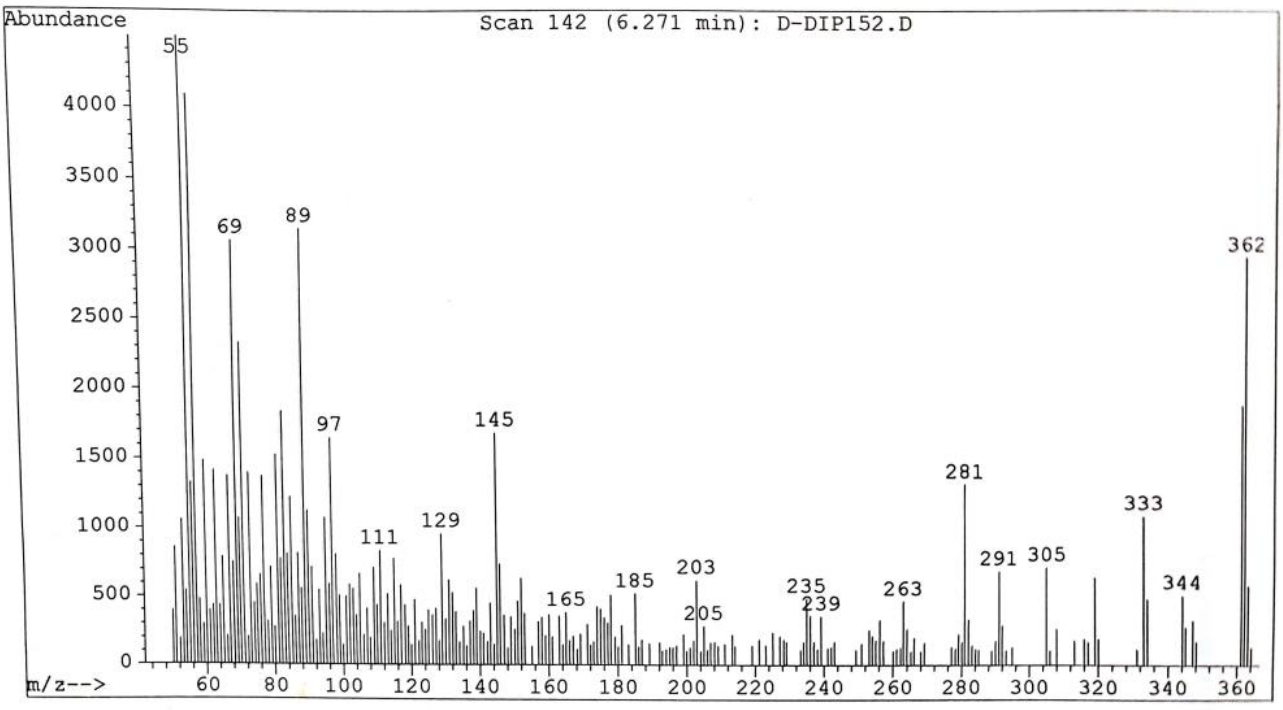

Figure 36 MS spectrum of compound 6j.

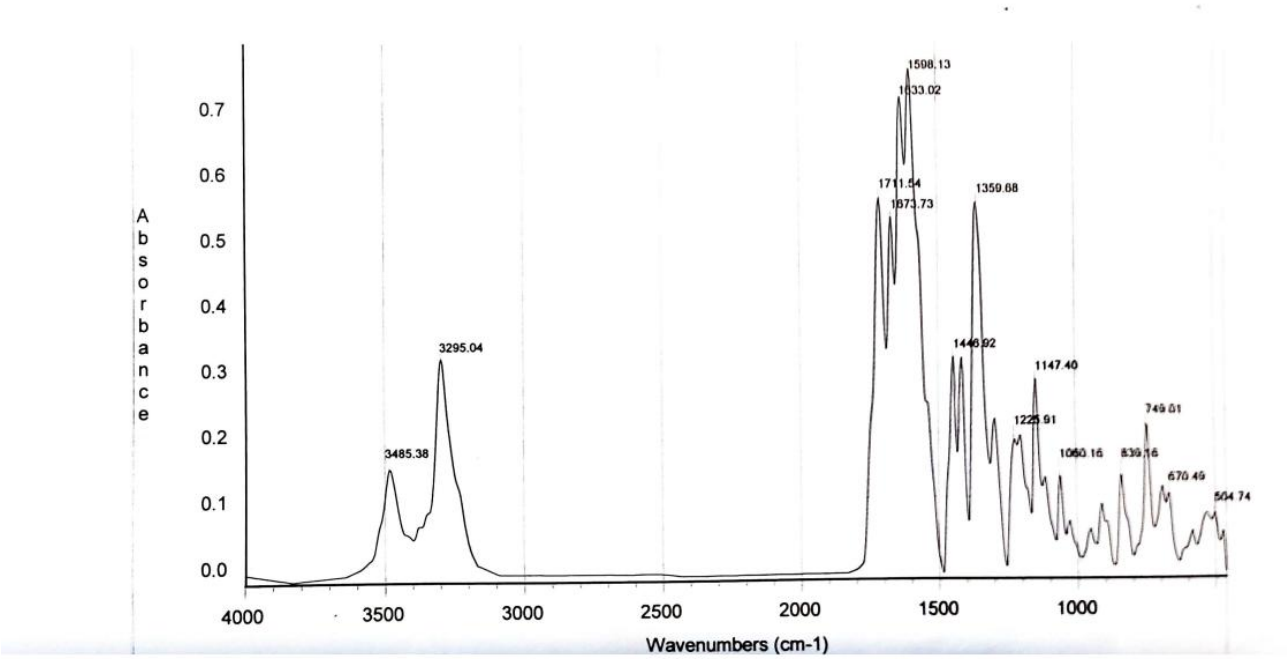

Figure 37 IR spectrum of compound 6k.

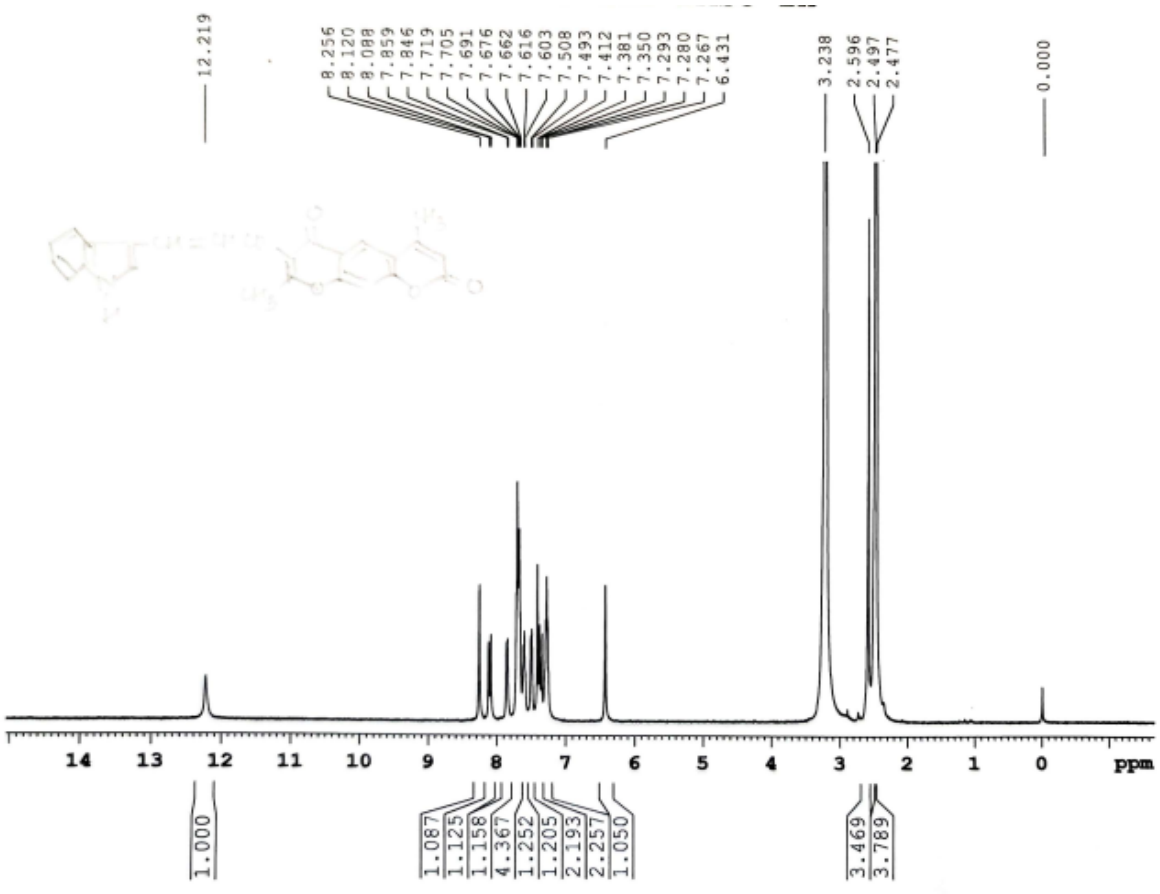

Figure 38 ^{1}H NMR spectrum of compound 6k.

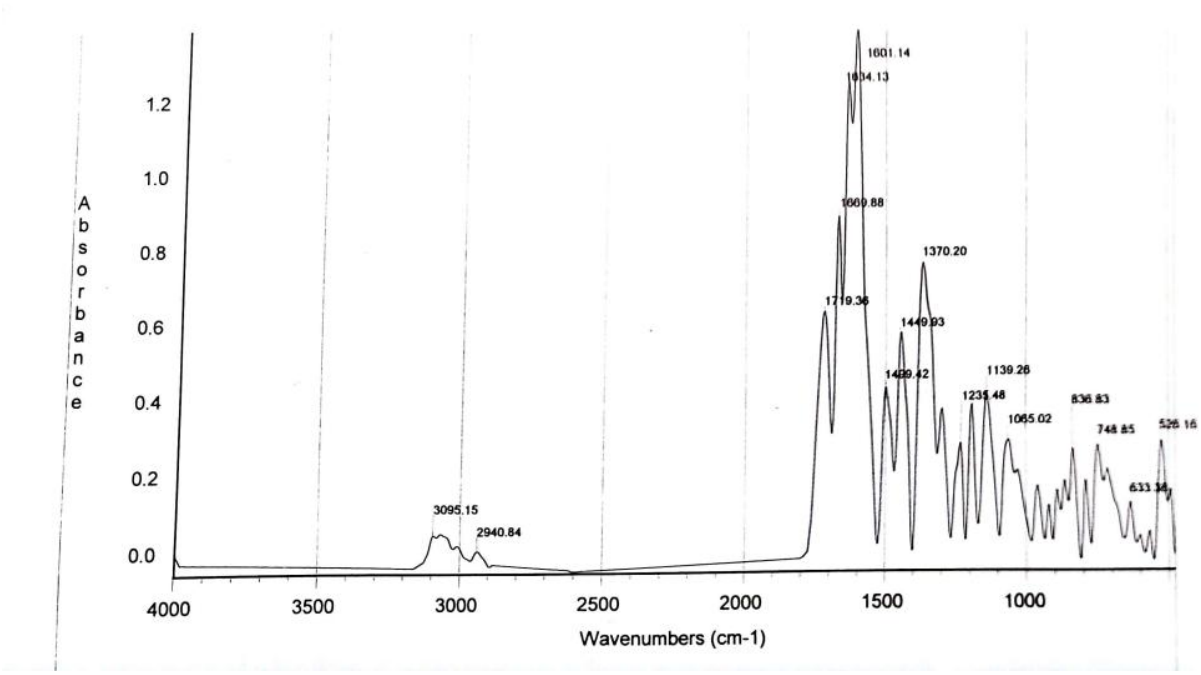

Figure 39 IR spectrum of compound 6l.

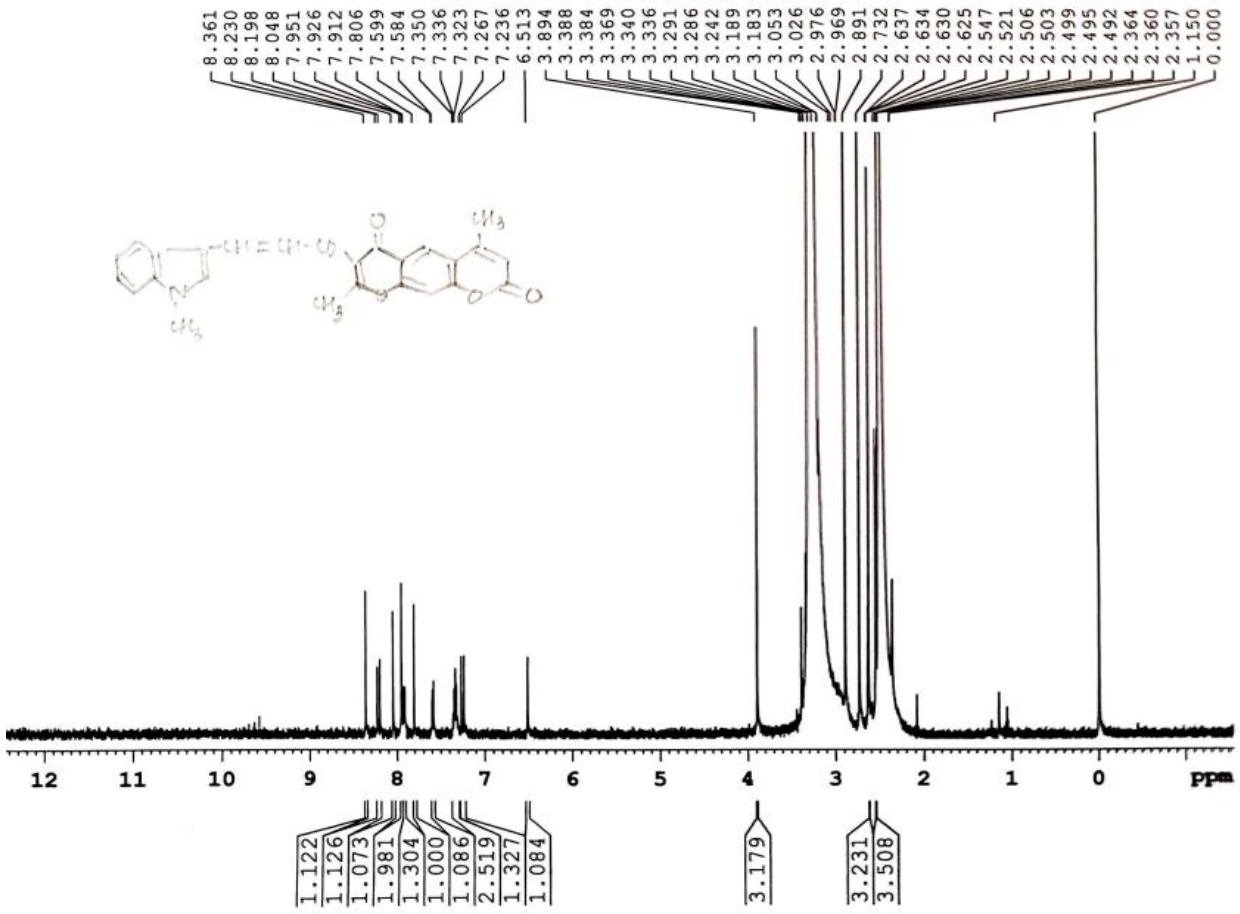

Figure 40 ^{1}H NMR spectrum of compound 6l.